

Chronic iEEG recordings and interictal spike rate reveal multiscale temporal modulations in seizure states

Gabrielle M. Schroeder¹, Philippa J. Karoly^{2,3}, Matias Maturana^{2,3}, Peter N. Taylor^{1,4,5},

Mark J. Cook², Yujiang Wang^{1,4,5*}

January 28, 2022

1. CNNP Lab (www.cnnp-lab.com), Interdisciplinary Computing and Complex BioSystems Group, School of Computing, Newcastle University, Newcastle upon Tyne, United Kingdom
2. Graeme Clark Institute and St Vincent's Hospital, University of Melbourne, Melbourne, Victoria, Australia
3. Department of Biomedical Engineering, University of Melbourne, Melbourne, Victoria, Australia
4. Faculty of Medical Sciences, Newcastle University, Newcastle upon Tyne, United Kingdom
5. UCL Queen Square Institute of Neurology, Queen Square, London, United Kingdom

* Yujiang.Wang@newcastle.ac.uk

1 Abstract

In focal epilepsy, various seizure features, such as spread and duration, can change from one seizure to the next within the same patient. Importantly, within-patient seizure evolutions do not change randomly over time, but instead appear to fluctuate over circadian and slower timescales. However, the specific timescales of this variability, as well as the specific seizure characteristics that change over time, are unclear.

Here we analysed this within-patient seizure variability in 10 patients with chronic intracranial EEG recordings (185-767 days of recording time, 57-452 analysed seizures/patient). We characterised the seizure evolutions as sequences of a finite number of functional network states. We then compared seizure state occurrence and seizure state duration to (1) time since implantation and (2) patient-specific circadian and multidien cycles in interictal spike rate, which were extracted using empirical mode decomposition.

In most patients, the occurrence or duration of at least one state was associated with the time since implantation (8 and 9 patients for state occurrence and state duration, respectively). Additionally, some patients also had one or more states that were associated with phases of circadian and/or multidien spike rate cycles (4 and 7 patients for state occurrence and state duration, respectively). A given state's occurrence and duration were not usually associated with the same timescale.

Our results suggest that time-varying factors modulate within-patient seizure evolutions over multiple timescales, with separate processes modulating a seizure state's occurrence and duration. These findings provide new insight into the patterns and mechanisms of intra-patient seizure variability, with potential implications for forecasting and treating seizures.

2 Introduction

Focal epilepsy is characterised by recurrent, unprovoked seizures. Importantly, these seizures are not homogeneous events, even in the same patient. Within individual patients, seizure features such as clinical symptoms (Noachtar and Peters, 2009), onset locations and patterns (Gliske et al., 2018; Jiménez-Jiménez et al., 2015; King-Stephens et al., 2015; Saggio et al., 2020; Salami et al., 2020), durations (Cook et al., 2016; Schroeder et al., 2021), and network evolutions (Schroeder et al., 2020) can change over time and potentially influence treatment responses (Cook et al., 2016; Ewell et al., 2015; Ryzi et al., 2015). As such, a better understanding of patterns and sources of within-patient seizure variability is needed.

One open question is whether and how such seizure features change over short (e.g., circadian) and long (e.g., weekly, monthly, and yearly) periods of time. There is some evidence that seizures are modulated over different timescales. For example, certain clinical seizure types and symptoms, such as secondary generalisation, can preferentially occur during certain parts of sleep/wake or day/night cycles (Bazil, 2018; Bazil and Walczak, 1997; Janz, 1962; Loddenkemper et al., 2011; Sinha et al., 2006). Electrographic seizure onset patterns can shift across the days of epilepsy monitoring unit (Gliske et al., 2018) and months of chronic intracranial EEG (iEEG) (Ung et al., 2016) recordings, suggesting that seizure features can also change over slower timescales. More recently, our preliminary analysis in epilepsy monitoring unit patients found that seizure network evolutions do not change randomly over time (Schroeder et al., 2020). Instead, over the timescales of these recordings, seizures with more similar network evolutions tended to occur closer together than less similar seizures. Further, in most patients, the changes in seizure network evolutions could be explained by a combination of circadian and/or slower time-varying factors. However, these temporal associations and the specific timescales of seizure changes need to be further explored in longer recordings with larger numbers of seizures.

In recent years, chronic iEEG recordings with durations of months to years have provided unprecedented insights into epileptic brain dynamics over multiple timescales (Cook et al., 2013; Davis et al., 2011; Howbert et al., 2014; Jarosiewicz and Morrell, 2021). First, these recordings have revealed shifts in interictal dynamics, including in the rates and spatial patterns of bursts (Ung

et al., 2016), spikes (Chen et al., 2021), high frequency activity (Chen et al., 2021), and other signal features (Ung et al., 2017). This variability is especially high in the first months after electrode implantation, possibly due to the brain’s response to acute trauma (Chen et al., 2021; Ung et al., 2016, 2017). However, more persistent variability in such features has also been observed (Chen et al., 2021; Ung et al., 2016), suggesting that other mechanisms also drive the observed interictal shifts. In addition, multiple studies have found prevalent patient-specific circadian, multidien, and/or circannual cycles in interictal features and seizure occurrence (Baud et al., 2018; Chen et al., 2021; Karoly et al., 2018a, 2021; Leguia et al., 2021; Maturana et al., 2020). Since the exact periods of these cycles often vary over time, they are best tracked using fluctuations in continuous biomarkers such as interictal spike rate (Baud et al., 2018; Leguia et al., 2021; Maturana et al., 2020). An intriguing possibility is that seizure features and seizure evolution could also change over the timescales of patient-specific cycles. For example, certain seizure features may occur preferentially at a particular phase, and other features may gradually change over the course of a spike rate cycle. However, the relationship between seizure features and spike rate cycles has not been explored.

In this work, we addressed these questions by analysing changes in seizure network evolutions in chronic iEEG recordings from the NeuroVista dataset (Cook et al., 2013). We described seizure evolutions as a sequence of a small number of patient-specific network states, similar to past studies (Burns et al., 2014; Khambhati et al., 2015). In each patient, we then analysed changes in seizure states over multiple timescales. We first identified gradual changes in seizures states across the course of each recording. We then determined if seizure states also fluctuated over patient-specific circadian and multidien cycles that were revealed by interictal spike rate. To account for possible independent variability in seizure evolutions and seizure duration (Schroeder et al., 2021), we separately examined variability in seizure state occurrence and seizure state duration. We show that in most patients, both of these features were associated with multiple timescales, providing new insight into the patterns and possible mechanisms of within-patient seizure variability.

3 Results

We analysed seizure network evolutions in 10 patients with focal epilepsy who underwent chronic continuous iEEG recordings as part of the NeuroVista seizure prediction study (Cook et al., 2013). Patient details are provided in Supplementary Table S1.1.

3.1 Seizure network evolutions vary from seizure to seizure within individual patients

In each patient, we first characterised changes in seizure network evolutions over the length of the patient’s continuous iEEG recording. Specifically, we described seizure network evolutions as a sequence, or progression, of network states (see Methods for details). Similar approaches have previously been used to summarise seizure network evolutions by characterising recurring elements of seizures (Burns et al., 2014; Khambhati et al., 2015). Fig. 1A shows these progressions for an example patient, NeuroVista 1. The vertical lines indicate seizures that occurred during the patient’s approximately two year recording. The colours of the lines indicate the network state in each seizure time window, with each time window corresponding to approximately a second of the iEEG recording. NeuroVista 1 had six seizure network states that each described a specific pattern of coherence between the patient’s iEEG channels (Supplementary section S2). These state progressions therefore summarise the evolution of channel interactions during the patient’s seizures. Although these states did not explicitly capture visual differences in seizure iEEG traces, seizures with different network evolutions also tend to have different electrographic patterns (Schroeder et al., 2020, 2021). As an example, Fig. 1B shows two seizures that began with the same three states (states B, E, and C), but had different final states (state D, dark blue, vs. state F, dark orange), at which time the amplitude and frequency of their seizure activity also diverged.

From Fig. 1A, it is already apparent that seizure network evolutions differed from seizure to seizure. In particular, there was variability in both state occurrence (i.e., whether a state occurred during a seizure) (Fig. 1C) and state duration (defined as the number of time windows a seizure spent in the given state) (Fig. 1D). For example, in NeuroVista 1, state D only occurred in about

6.4 % of seizures, and, in those seizures, its duration could range from 8 to 52 windows.

Across patients, we also observed variability in seizure network state progressions (Fig. 1E,F), although the patterns of variability varied from patient to patient (see Zenodo Data File 10.5281/zenodo.5910238 for seizure state progressions of all patients). Importantly, seizure states are not comparable across patients due to patient-specific iEEG implantations; however, for convenience, we allow states in different patients to share the same letter label and colour. All patients had variability in state occurrence for the majority of their seizure states (Fig. 1E); indeed, only NeuroVista 6 and NeuroVista 9 had any states that occurred in all of their recorded seizures (two states and one state, respectively). Further, all seizure states had variable duration, indicating that state durations were not a fixed feature across seizures (Fig. 1F). Thus, both state occurrence and state duration captured information about within-patient seizure variability in our cohort, and we therefore investigated patterns of variability in both features. State occurrence is a binary feature that described whether or not the state occurred in a seizure. Meanwhile, state duration is a continuous measure that, in seizures containing the state, captured how long the state persisted.

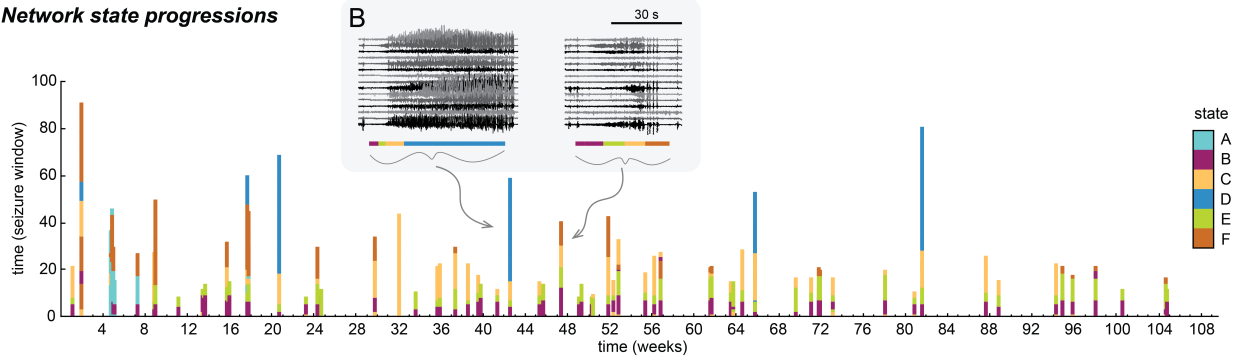
3.2 Seizure states vary over the duration of chronic iEEG recordings

We first asked if within-patient seizure state occurrence and duration varied over the timescale of each patient’s chronic iEEG recording. Specifically, we explored whether seizures that occurred early in the recording had different features from those seizures that occurred later.

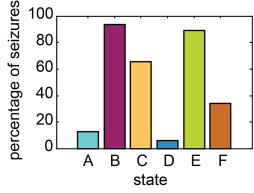
We first investigated relationships between the amount of time elapsed since implantation and seizure state occurrence. In each patient and for each of the patient’s seizure states, we divided the patient’s seizures into two groups: seizures containing the state and seizures that did not contain the state. We then compared the recording times (i.e., time since implantation) of these two groups. Fig. 2A shows the relationship of an example state with recording time. In this patient, NeuroVista 13, the prevalence of state C gradually increases over the recording period. While few seizures contain state C during the first few months of the recording, state C is present in the majority of seizures by the end of the recording. The temporal separability of seizures with and without state C can be characterised by the area under the curve (AUC) of distinguishing state

NeuroVista 1

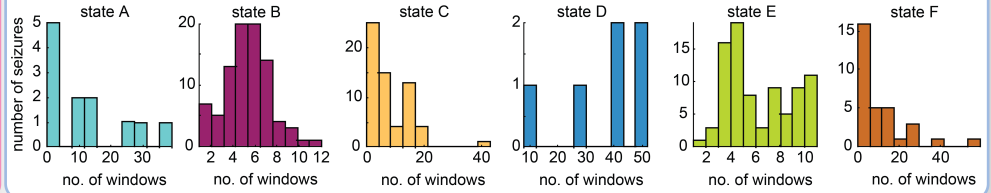
A Network state progressions



C Variability in state occurrence

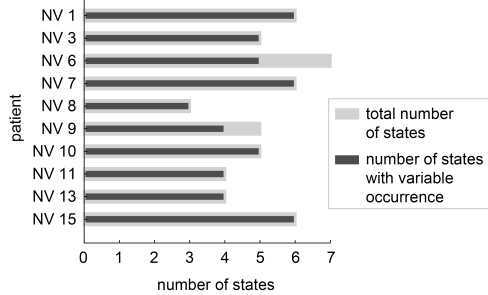


D Variability in state duration



All patients

E Variability in state occurrence



F Variability in state duration

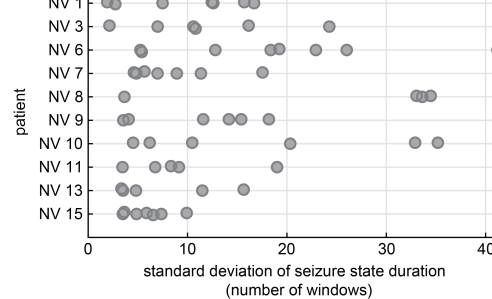


Figure 1: Variability in seizure network state progressions. Example patient, NeuroVista 1: A) Seizure network state progressions. Each seizure is represented by a vertical bar; its horizontal location indicates the time of seizure occurrence and the length of the bar indicates the seizure's duration in terms of the number of time windows (approximately equal to number of seconds). The colours of the bar indicate the network state of the seizure during each time window. B) The iEEG traces of two example seizures, with the seizures' network state progressions shown underneath. C) Percentage of NeuroVista 1's seizures that contained each seizure network state. D) Histograms of state durations of each of NeuroVista 1's network states. Seizures that do not contain a given state are excluded from the corresponding histogram (i.e., a state duration of zero is not included in the distribution). Across all patients: E) The number of seizure states in each patient (light gray bars), with the number of those states that had variable occurrence (i.e., did not occur in all of the patients seizures) overlaid with dark gray bars. F) Variability in seizure state duration for each patient's states. Each dot corresponds to a single seizure state. NV = NeuroVista.

occurrence based on seizure time, with an AUC below 0.5 indicating that the state preferentially occurs in earlier seizures and an AUC above 0.5 revealing that the state tends to occur in later seizures. Here, state C has an AUC of 0.71, which was significant after false discovery rate (FDR) correction for multiple comparisons (Wilcoxon rank-sum test, $p = 2.1 \times 10^{-12}$).

Across our cohort, eight out of the ten patients had at least one seizure state whose occurrence was significantly associated with the time since implantation after FDR correction for multiple comparisons (Fig. 2B). Ten states had AUCs greater than 0.5, while eight states had AUCs less than 0.5, revealing that a state’s occurrence can increase or decrease across a recording. Most states occurred across the majority of the recording (Supplementary S4), indicating that the observed temporal associations were not driven by transient states that only occurred during the initial part of the recording. Instead, the pool of possible states remained relatively consistent across a recording, but the likelihood of observing each state changed over time, as in Fig. 2A.

In the previous section, we observed that seizures with the same states can additionally differ due to variable amounts of time spent in those states (Fig. 1D,F). We therefore next investigated whether seizure state duration was associated with time since implantation. For each state, we only analysed state duration in seizures containing the state, thus ensuring that our results were not driven by seizures without the state (i.e., where state duration would be zero). In NeuroVista 15, state D demonstrates how seizure state duration can vary over the length of the recording (Fig. 3A). Here, state D’s duration is significantly higher in earlier seizures, as demonstrated by a significant Spearman’s correlation ρ of -0.59 after FDR correction for multiple comparisons ($p = 2.4 \times 10^{-6}$).

Almost all patients had at least one state whose duration was either significantly positively (eight states) or negatively (eight states) correlated with time since implantation (Fig. 3B-C) after FDR correction for multiple comparisons. Thus, seizure state duration can either increase or decrease across a patient’s chronic iEEG recording.

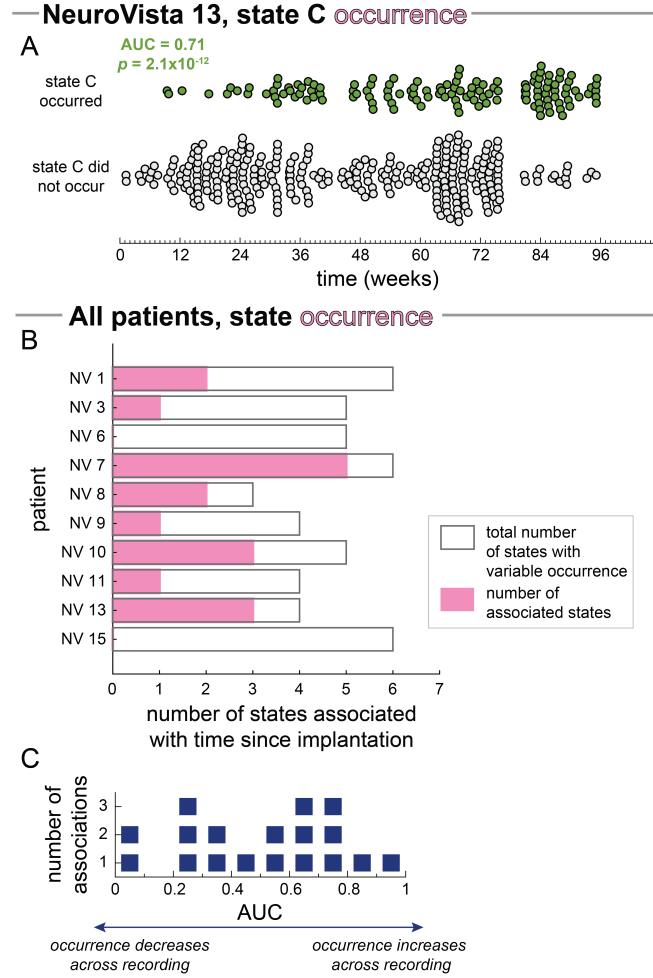


Figure 2: Relationship between seizure state occurrence and time since implantation. A) Times since implantation of seizures with (green circles) and without (grey circles) state C in example patient NeuroVista 13. Points are spread vertically to prevent overlap of seizures with similar times. Time since implantation separated seizures with and without state C with an AUC of 0.71. B-C) All patients: B) Number of seizure states whose occurrence was significantly associated with time since implantation in each patient (pink bars). Grey outlines provide a reference for the maximum possible number of associated states (i.e., the number of states with variable occurrence, equivalent to the dark grey bars in Fig. 1E). C) Dot plot of the AUCs for each significant state in (B). Each blue marker corresponds to one state.

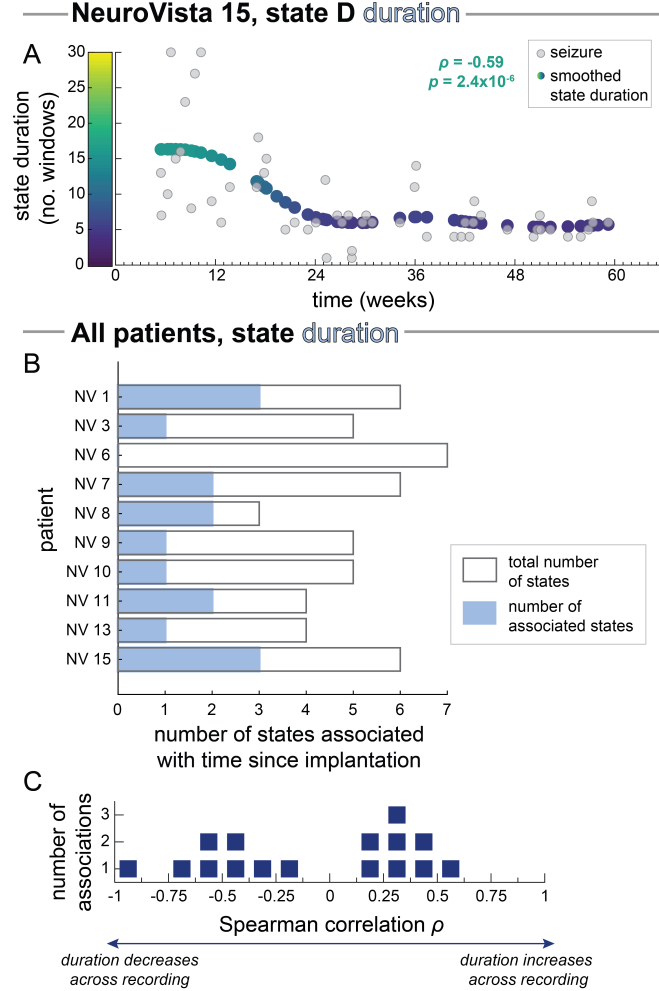


Figure 3: Relationship between seizure state duration and time since implantation. A) In example patient NeuroVista 15, state D duration versus the time since implantation, with a smoothed trend line (Gaussian window of 24 weeks) shown with the coloured points. Each grey point corresponds to a seizure that contained state D. B-C) All patients: B) Number of seizure states whose duration was significantly associated with recording time in each patient (light blue bars). Grey outlines provide a reference for the maximum possible number of associated states (i.e., the total number of states in each patient, equivalent to the light grey bars in Fig. 1E). C) Dot plot of the Spearman's correlation between state duration and recording time for all significantly associated states. Each blue marker corresponds to one state.

3.3 Seizure states fluctuate over circadian and multidien cycles

The previous results revealed seizure evolutions can differ across the multiple months of chronic iEEG recordings. However, we also hypothesised that seizure evolutions, like seizure occurrence (Baud et al., 2018; Karoly et al., 2021; Leguia et al., 2021; Maturana et al., 2020), may vary cyclically over circadian and multidien cycles. Importantly, these cycles can be nonstationary, with the cycle period varying over time; thus, they must be extracted using a continuous biomarker such as interictal spike rate (Baud et al., 2018; Karoly et al., 2021; Leguia et al., 2021; Maturana et al., 2020). We therefore next explored whether seizure state occurrence and duration were also be associated with interictal spike rate cycles.

As in previous work (Baud et al., 2018; Karoly et al., 2016, 2021; Leguia et al., 2021; Maturana et al., 2020), we observed high levels of variability in interictal spike rate across each patient’s chronic iEEG recording (see Fig. 4A for interictal spike rate of an example patient, NeuroVista 1). We obtained each patient’s interictal spike times from a previous study (Karoly et al., 2016) and used a data-driven approach, empirical mode decomposition (EMD) (Colominas et al., 2014; Huang et al., 1998), to extract fluctuations in spike rate over different timescales (see Methods for details and Zenodo Data File 10.5281/zenodo.5910238 for spike rate decompositions of all patients). EMD decomposes a time series into a series of oscillatory components that can have variable amplitude and frequency, thus accommodating non-stationarity in the spike rate cycles. To ensure that the extracted cycles were robust, we limited our analysis to the most prominent cycles that also had average periods of a quarter or less of the length of the patient’s recording (see Methods for details). Fig. 4B shows the extracted spike rate cycles of NeuroVista 1. Their fastest cycle (yellow) was circadian, with an average period of 0.96 days. The patient also had a multidien cycle (red) of approximately 10.61 days. These spike rate cycles captured different timescales of changes in spike rate in NeuroVista 1’s recording. We observed such multiscale fluctuations in interictal spike rate in most patients (Fig. 4C, see Supplementary section S3 for selection of spike rate timescales). All patients had prominent circadian cycles in spike rate (average period of 0.84-1.02 days), and eight of the ten patients also had at least one multidien cycle, with average periods ranging from 3.60 to 54.77 days. Together, these cycles characterised the prominent patient-specific, non-stationary

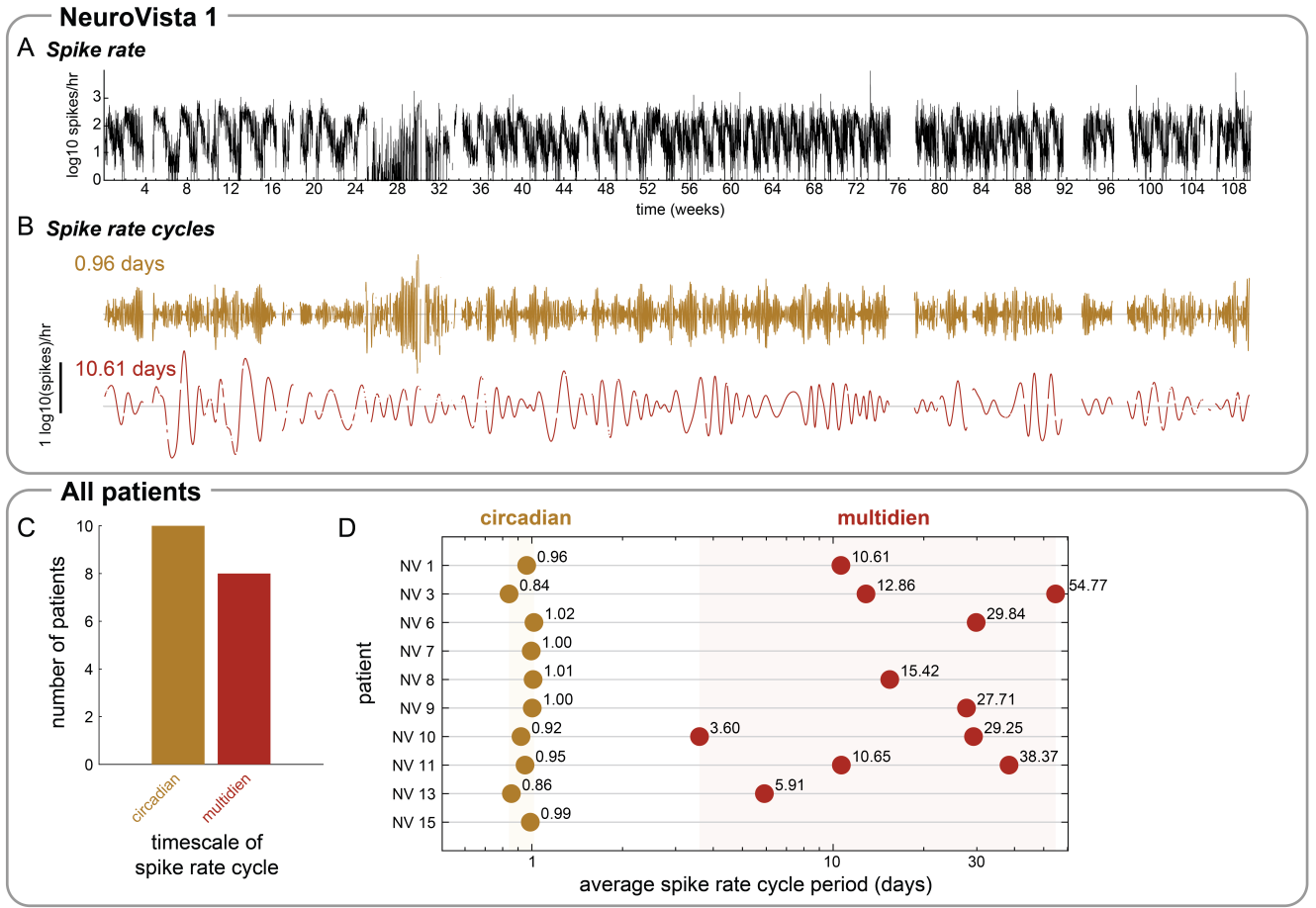


Figure 4: Patient-specific cycles in interictal spike rate. A-B) Example subject NeuroVista 1: A) The interictal spike rate (spikes per hour) during NeuroVista 1’s recording. B) The two prominent cycles in NeuroVista 1’s spike rate, extracted using empirical mode decomposition (EMD). NeuroVista 1 had a circadian (average period of 0.96 days) and multidien (average period of 10.61 days) cycle. C-D) All patients: C) Number of patients that had at least one spike rate cycle at each timescale. D) Spike rate cycles of each patient, coloured by their timescale.

changes in spike rate in each patient.

For each patient, we first asked whether seizure states preferentially occurred during certain phases of each spike rate cycle. Similar to previous work (Baud et al., 2018; Karoly et al., 2018a; Leguia et al., 2021), we defined phase preference as the phase locking value (PLV) of a state for a spike rate cycle. A PLV of 0 would indicate that the state had no phase preference, while a PLV of 1 would indicate that the state only occurred at one phase of the cycle. Importantly, seizures themselves would likely show phase preferences for some of the spike rate cycles (Baud et al., 2018; Karoly et al., 2021; Leguia et al., 2021; Maturana et al., 2020), which would by proxy lead to phase preferences for seizure states as well. Therefore, to control for seizure timing phase

preferences, we used permutation tests to determine the significance of the state occurrence PLV. In other words, we determined if a separate phase preference existed for each seizure state, beyond the phase preference of the seizures.

Fig. 5A-C shows an example of a seizure state, state F, that preferentially occurred during certain phases of NeuroVista 1’s multiday spike rate cycle. In this example, state F was mostly likely to occur during a specific part of the rising phase of the multiday cycle, with the proportion of seizures with this state tapering towards the cycle peak. Further, almost all seizures that occurred during the falling phase and the cycle trough lacked this state. As such, state F’s PLV was significantly stronger than the overall seizure PLV (state PLV = 0.84, +0.21 relative to PLV of all seizures, $p = 0.0014$) after FDR correction for multiple comparisons.

Across our cohort, four patients (NeuroVista 1, 7, 10, and 13) had at least one seizure state whose occurrence was significantly associated with a spike rate cycle after FDR correction for multiple comparisons (Fig. 5D-E). Note that the same state could be associated with multiple different spike rate cycles (Supplementary section S5). Four of these patients had a state that had a phase preference to their circadian cycle, while two patients had one or more states associated with at least one multidienn cycle (Fig. 5F). We also quantified the strength of the significant associations with spike rate cycles by computing the state PLV increases relative to the overall PLV of all seizures for the given cycles (Fig. 5G). The increase in PLV varied from 0.07-0.22, with most states showing a weak increase in PLV (median: 0.12). We interpret these associations as evidence that, in some patients, certain spike rate cycles reveal a modulation in seizure state occurrence over a specific timescale.

We then investigated if seizure state duration also varies over seizure cycles. For seizures with a given state, we computed the rank circular-linear correlation D (Mardia, 1976) between the seizures’ state durations and the phases of the spike rate cycle at which the seizures occurred, using permutation tests to determine statistical significance (see Methods). The measure D is not signed, but instead ranges from 0 to 1, with zero indicating no association. Seizures without the state (i.e., with a state duration of zero) were excluded from the analysis so that duration results were not driven by state occurrence phase preferences.

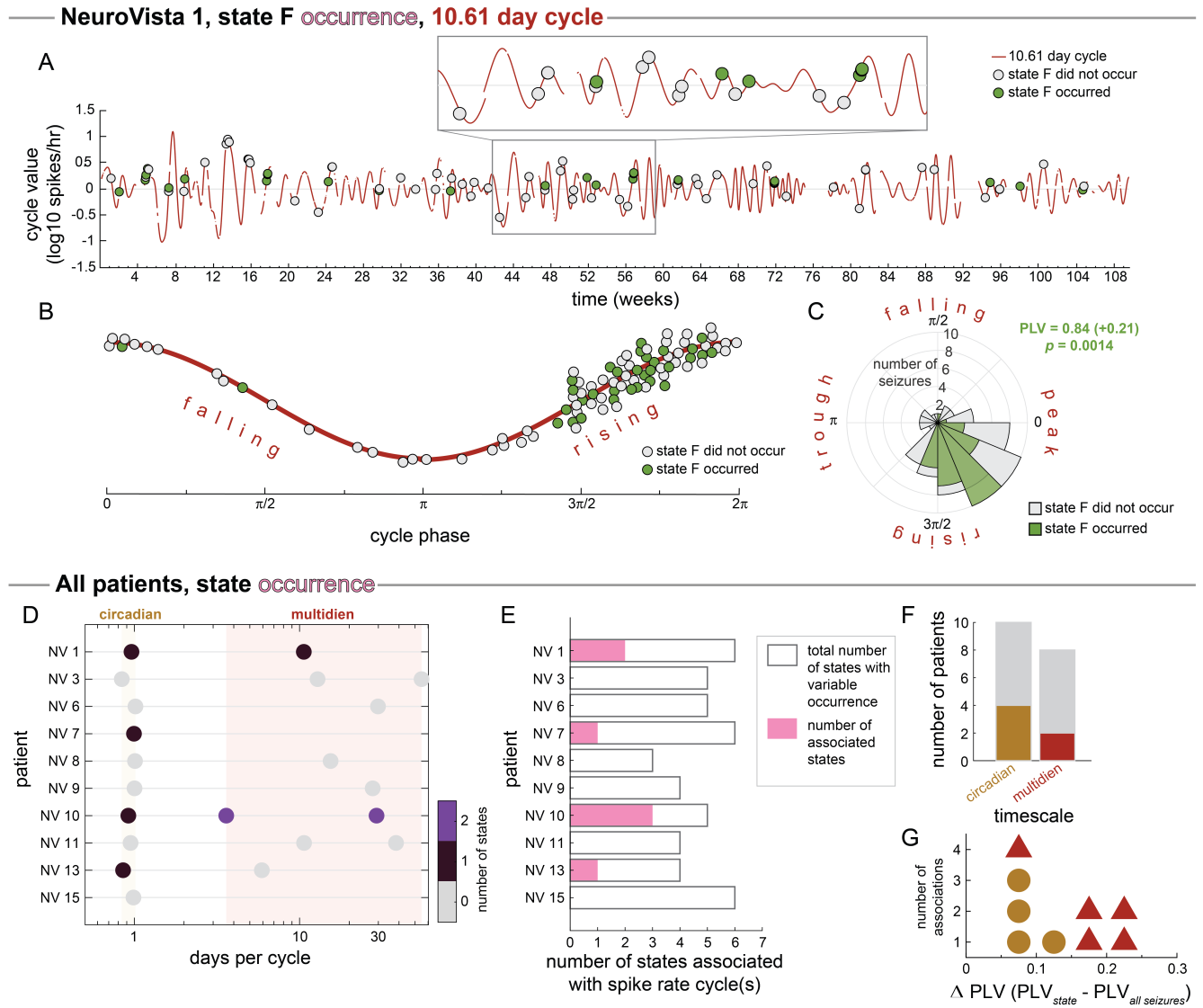


Figure 5: Associations of seizure state occurrence with spike rate cycles. NV = NeuroVista. A-C) Example subject NeuroVista 1, seizure state F, 10.61 day cycle: A) NeuroVista 1's 10.61 day spike rate cycle versus time, with seizures (circles) overlaid on the cycle at the times they occurred. Circles are coloured by whether the seizure did (green) or did not (grey) contain state F. The boxed inset expands a part of the cycle. B) Representation of the phase of the 10.61 day cycle, with the curve indicating whether spike rate is falling or rising at the given phase. As in A, circles correspond to seizures with (green) and without (grey) state F, and they are plotted on the curve at the phase that they occurred. Seizure circles are spread vertically to show all circles. C) Polar histogram of seizure phases with (green) and without (grey) state F. D-G) All patients: D) Coloured circles indicate the spike rate cycles. The circle colours correspond to the number of states significantly associated with the patient's spike rate cycle at that timescale. Grey circles indicate that the patient had a spike rate cycle at that timescale, but that that timescale was not associated with the occurrence of any seizure state. E) Total number of seizure states associated with spike rate cycles in each patient. Grey outlines provide a reference for the maximum possible number of associated states (i.e., the number of states with variable occurrence). F) For each timescale of spike rate cycle, the number of patients that had at least one state associated with that timescale. Grey bars indicate the number of patients with each timescale (equivalent to the coloured bars in 4C). G) Dot plot of the strength of the phase preferences of significantly associated states, measured as changes in PLV (state PLV minus the PLV of all seizures for the associated spike rate cycle). Marker shape and colour indicates the timescale category of the associated spike rate cycle.

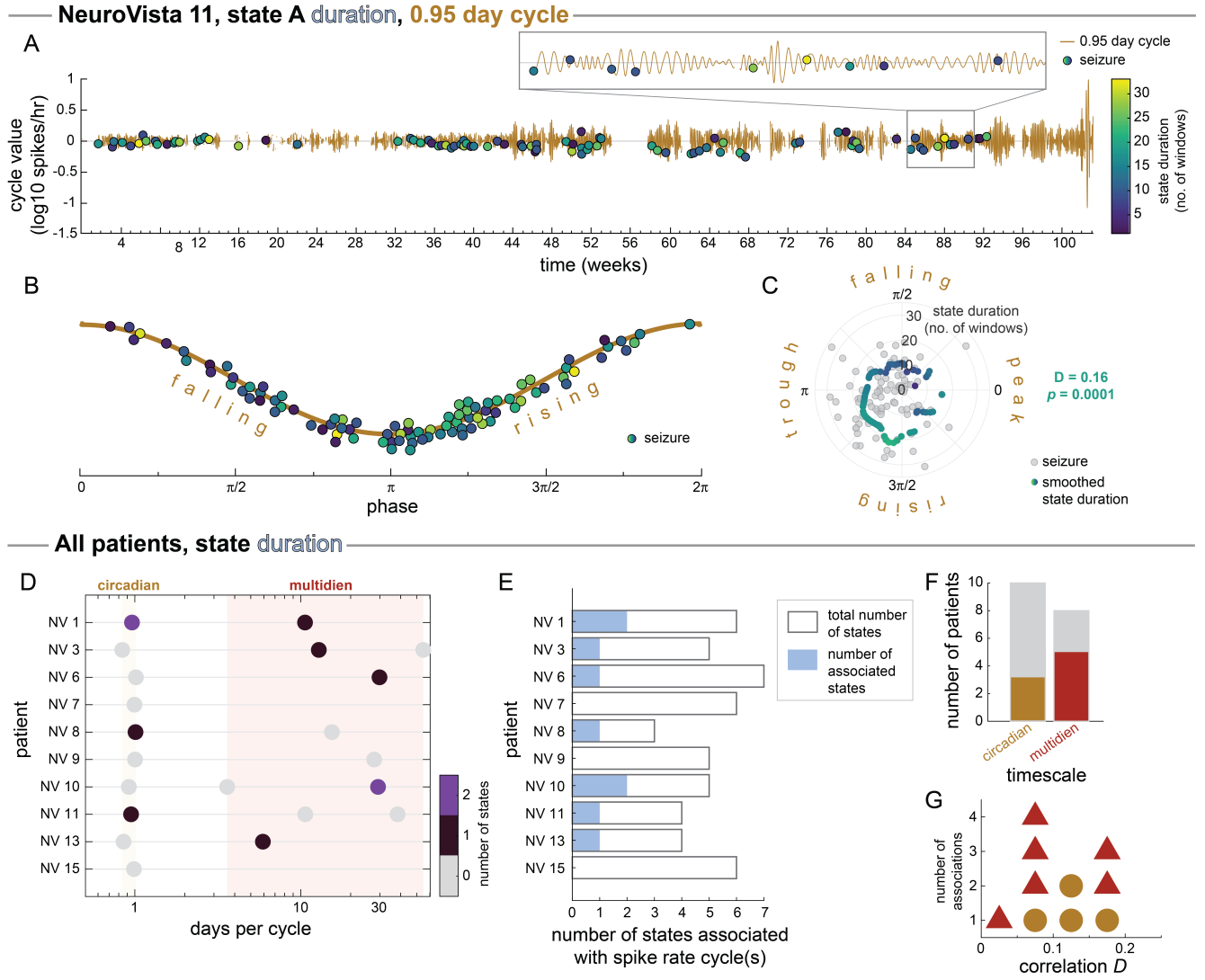


Figure 6: Associations of seizure state duration with spike rate cycles. NV = NeuroVista. A-C) NeuroVista 11, seizure state A, 0.95 day spike rate cycle: A) The circadian spike rate cycle versus time, with seizures containing state A (circles) overlaid on the cycle at the times they occurred. Circles are coloured by state duration. The boxed inset expands a part of the cycle. B) Representation of the phases of the spike rate cycle, with the curve indicating whether spike rate was falling or rising at the given phase. As in (A), circles correspond to seizures with state A, with their colour indicating state duration. Seizure circles are spread vertically to show all circles. C) Polar scatter plot of state duration versus seizure phase. Each grey point indicates a seizure, while coloured points correspond to the smoothed seizure duration ($\pi/4$ Gaussian window). D-G) All patients: D) Coloured circles indicate the spike rate cycles in each patient. The colours of the circles indicate the number of states significantly associated with the patient's spike rate cycle at that timescale. Grey circles indicate that the patient had a spike rate cycle at that timescale, but that that cycle was not associated with the duration of any seizure state. E) Total number of seizure states whose durations were associated with spike rate cycles in each patient. Grey outlines provide a reference for the maximum possible number of associated states. F) The number of patients that had at least one state duration associated with a spike rate cycle at each timescale. Grey bars indicate the number of patients with each timescale (equivalent to the coloured bars in 4C). G) Dot plot of the strengths of the significant associations between state duration and spike rate cycle phases, measured as non-parametric circular-linear correlation D . Marker shape and colour indicates the timescale category of the associated spike rate cycle.

Fig. 6A-C shows an example seizure state duration association with a spike rate cycle in NeuroVista 11. In this patient, the circadian spike rate cycle was significantly associated with the duration of state A after FDR correction for multiple comparisons ($p = 0.0001$). State A’s duration was markedly higher during the rising phase than during the falling phase of the spike rate cycle (Fig. 6B); the average duration starts increasing shortly before the trough of the cycle and peaks at approximately $3\pi/2$ in the rising phase before decreasing again (Fig. 6C).

In our cohort, seven patients had one or more states whose duration was significantly associated with spike rate cycle phases (Fig. 6D-E). As with seizure state occurrence, we interpret these associations as evidence that seizure state duration can be modulated over various timescales of spike rate cycles. Circadian and multidien cycles were associated with state duration in three and five patients, respectively. The strength of the correlations between seizure state duration and spike rate cycle phases varied from 0.04 to 0.18, with most state durations showing a weak correlation with spike rate phase (median: 0.09).

3.4 A seizure state’s occurrence and duration are usually independently modulated

In previous work, we found that seizure duration could vary independent of changes to the seizure’s network evolution (Schroeder et al., 2021). Thus, two seizure with the same sequence of states could have different durations due to temporal “elasticity,” which results in one seizure dwelling for longer in a particular state. We therefore next asked whether a given state’s occurrence and duration were associated with the same timescale, which we interpret as co-modulation by the same fluctuation/process.

In each patient, we first determined whether each seizure state’s 1) occurrence, but not duration, was associated with the time since implantation, 2) duration, but not occurrence, was associated with the time since implantation, or 3) occurrence and duration were both associated with time since implantation. Fig. 7A shows the number of states in each patient that belonged to each category. Although the occurrence and duration of the same state were sometimes both associated with time since implantation, it was more common for only one feature of a state to be associated.

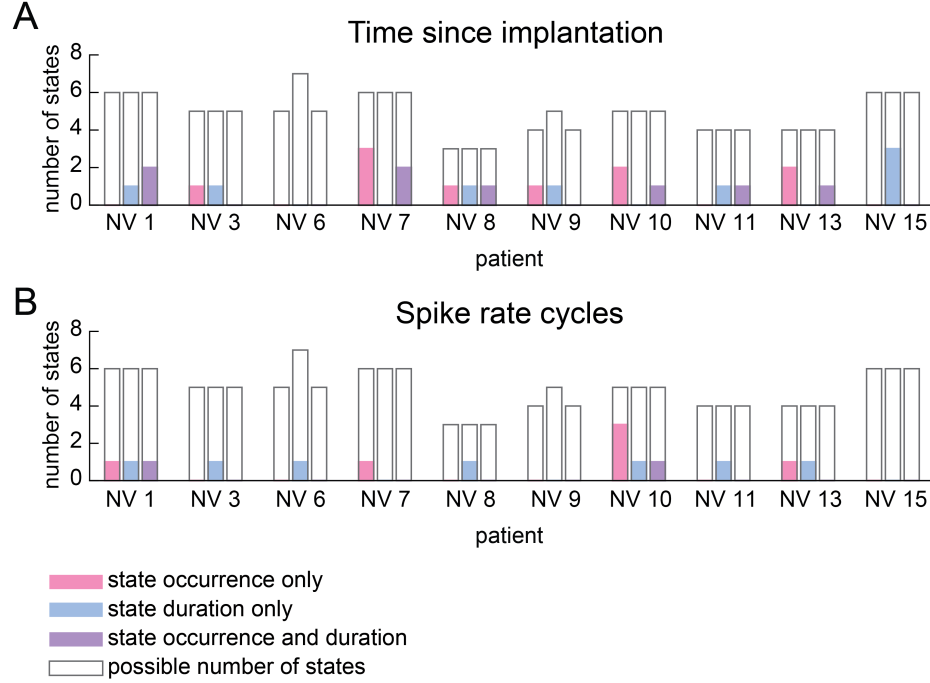


Figure 7: Independent and coinciding timescales of seizure state occurrence and duration modulation A) From left to right, the three bars for each patient show the number of the patient's seizure states in which 1) only state occurrence was associated with time since implantation (pink), 2) only state duration was associated with time since implantation (blue), and 3) occurrence and duration were both associated with time since implantation (purple). Grey outlines provide a reference for the maximum number of states that can belong to each category (i.e., for occurrence counts, the number of seizures states with variable occurrence, and for duration counts, the total number of seizures states) in each patient. B) Same measures as A for state associations with spike rate cycles.

We repeated this analysis for seizure state associations with spike rate cycles (Fig. 7B). Note that for this analysis, a state could belong to multiple categories if its occurrence and duration were associated with different spike rate cycles; for example, a state’s occurrence could be associated with a circadian cycle (category 1) while its duration could vary over a multidien cycle (category 2). For spike rate timescales, a state’s occurrence and duration were only associated with the same timescale in one state in NeuroVista 1 and one state in NeuroVista 10 (Supplementary section S5). Thus, joint modulation of state occurrence and duration was rare over circadian and multidien timescales.

Finally, we investigated two relationships to support our overall results. First, we analysed whether certain parts of a seizure (e.g., onset states) were more likely to change over a given timescale. For both state occurrence and state duration, we did not find any significant associations between where the state occurred in the seizure evolution and whether the state was associated with the time since implantation or a spike rate cycle (Supplementary S6). These results indicate that multiple places in seizure evolutions are susceptible to temporal modulation. Second, we investigated whether total seizure duration was associated with the time since implantation and spike rate cycles (Supplementary section S5). We observed associations with total state durations in only a few patients, indicating that overall changes in seizure duration were not the sole driver of our observed state duration associations. In other words, seizure state durations did not simply vary due to changes in overall seizure duration, where increasing seizure duration proportionally increased the component states’ durations. This observation supports our earlier hypothesis that specific parts of seizure evolutions may be more prone to temporal “elasticity” (Schroeder et al., 2021; Wenzel et al., 2017), or variable duration.

4 Discussion

We analysed variability in seizure network state progressions in chronic iEEG recordings, providing novel insight into the patterns and mechanisms of seizure variability. We found that in most patients, seizure states depended on when the seizure occurred in the recording, with some states becoming more or less prevalent and/or increasing or decreasing in duration as the recording pro-

gressed. Additionally, several patients had one or more states associated with circadian and/or multidien cycles in interictal spike rate. These associations suggest that seizure features are modulated over multiple timescales, including circadian and multidien timescales that can be revealed by interictal biomarkers.

We first found that seizure evolutions often depended on the amount of time that had elapsed since the start of the patient’s recording. Variability over such long timescales (multiple months to years) may reflect non-cyclical changes in seizure evolutions due to factors such as postimplantation effects (Chen et al., 2021; Ung et al., 2016, 2017), medication changes (Napolitano and Orriols, 2013), and slow changes in the epileptic network due to plasticity (Hsu et al., 2008). Alternatively, more gradual changes in seizure evolutions could be produced by cycles with long periods relative to the length of these recordings. Analysing longer recordings could determine if persistent seizure variability reflects longer cycles, such as circannual cycles, in brain dynamics (Karoly et al., 2021; Leguia et al., 2021; Rao et al., 2020). Notably, transiently observed states at the beginning of recordings were uncommon in our cohort, suggesting that implantation effects rarely cause atypical seizure states. Thus, shorter presurgical recordings patients with epilepsy, which typically last for a few days to a few weeks, likely contain a patient’s usual seizure states, although state duration and relative state prevalence may change over time. However, some additional seizure states may emerge after weeks of recording (King-Stephens et al., 2015; Ung et al., 2016) that would therefore be missed during presurgical monitoring. Thus, uncovering the longer timescales of variability in seizure evolutions has important implications for interpreting shorter iEEG recordings. Our findings add to the existing literature on variability in brain dynamics across chronic iEEG recordings (Chen et al., 2021; Ung et al., 2016, 2017) by revealing that multiple features of seizure evolutions also vary across these longer timescales.

We also observed associations between seizure state variability and circadian and/or multidien cycles in several patients. It is well-known that there are also cycles in seizure occurrence over the same timescales (Gowers, 1885; Karoly et al., 2016, 2018a; Langdon-Down and Brain, 1929; Loddenkemper et al., 2011; Navis and Harden, 2016; Patry, 1931), and recent research has revealed that fluctuations in interictal spike rate can serve as a biomarker for these seizure cycles

(Baud et al., 2018; Karoly et al., 2021; Leguia et al., 2021; Maturana et al., 2020). We previously found evidence of circadian rhythms in seizure evolutions from short-term epilepsy monitoring unit recordings, and the same results suggested that slower trends also modulated seizure dynamics (Schroeder et al., 2020). Here, we confirmed that seizure features follow both circadian and multi-day cycles that are linked to fluctuations in interictal spike rate. Compared to our previous study (Schroeder et al., 2020), our work here uses much longer recordings and larger numbers of seizures per patient, providing new evidence for time-varying modulation of seizure evolutions. Moreover, we identify specific aspects of seizure evolutions, network state occurrence and network state duration, that change over time in most patients. Our results reveal that there is a multiscale temporal structure to seizure variability, and certain characteristics of seizures are susceptible to modulation over a specific timescale.

We found that both seizure state occurrence and seizure state duration changed over the duration of the recording and were associated with spike rate cycles. Interestingly, a given seizure state’s occurrence and duration were usually not associated with the same timescale, indicating that these features were modulated separately in most patients. This finding suggests that the absence of a state is not a special case of duration variability where the state’s duration is zero. Additionally, it implies that a state’s duration is not necessarily linked to its likelihood of occurring in the seizure; for example, a state does not necessarily persist for longer in seizures where the state is more likely to occur. Instead, separate factors appear to control whether a seizure state occurs and the duration of the state when it occurs. Additionally, we observed that the durations of specific seizure states, had associations with time since implantation and spike rate cycles. This observation supports our earlier hypothesis that specific parts of seizure evolutions may be more prone to temporal “elasticity” (Wenzel et al., 2017), or variable duration (Schroeder et al., 2021). We suggest that future research on seizure duration variability likewise decompose seizure evolutions into states or other subparts to uncover factors that impact overall seizure duration.

Our work builds on past research that provided evidence for seizure variability over specific timescales. For example, it is well-established that in some patients, clinical seizure features such as secondary generalisation are associated with sleep/wake state or day/night cycles (Bazil, 2018;

Bazil and Walczak, 1997; Janz, 1962; Loddenkemper et al., 2011; Sinha et al., 2006). Past analysis of chronic iEEG in canines also discovered shifts in seizure onset patterns as the recording progressed, likely due to postimplantation variability in brain dynamics (Ung et al., 2016). Additionally, variability in seizure onset and spread have been linked to preictal and interictal changes in network features (Khambhati et al., 2016), band power (Naftulin et al., 2018), the location of high frequency oscillations (Gliske et al., 2018), and patterns of cortical excitability (Badawy et al., 2009). The same interictal features (network dynamics (Kuhnert et al., 2010; Mitsis et al., 2020), band power (Panagiotopoulou et al., 2021), high frequency activity (Chen et al., 2021), and cortical excitability (Meisel et al., 2015)) have all been shown to vary over circadian and/or multidien cycles. We now show that seizure evolutions also change over the timescales that influence interictal brain dynamics, suggesting that these fluctuations share common mechanisms.

Our analysis of circadian and multidien timescales of seizure variability relied on identifying cycles in interictal spike rate. To extract spike rate cycles, we used a data-driven method, EMD, that is adept at decomposing non-stationary time series (Huang et al., 1998). We additionally used a variation of EMD that improves the separation of cycles with different frequencies (Colominas et al., 2014). Unlike approaches such as wavelet decomposition, EMD does not require hypotheses about cycle frequencies or shapes, as cycles are instead found using the intrinsic fluctuations of the time series. EMD is also unique due to its iterative approach for extracting different timescales of cycles. This method provides advantages for spike rate analysis: the spike rate time series does not need to be smoothed to extract slower cycles, and cycles with drastically different periods can be uncovered without scanning a wide range of possible cycle frequencies. Although EMD differs from previous approaches for finding spike rate cycles (Baud et al., 2018; Karoly et al., 2018a; Leguia et al., 2021; Maturana et al., 2020), we found similar results, including circadian spike rate cycles in every patient as well as many multidien cycles. To increase confidence in our extracted spike rate cycles, we also limited our analysis to the cycles that persisted across the recording and had relatively high contributions to the overall spike rate. Future work could use a less conservative approach and determine if less salient cycles also influence seizure evolutions.

Although we found many associations between seizure timing, spike rate cycles, and seizure

states, we were unable to explain the full spectrum of seizure variability in our patients. Other approaches could yield more comprehensive and stronger explanations of seizure features. First, our analysis focused on spike rate phase due to its association with seizure occurrence (Baud et al., 2018; Karoly et al., 2021; Leguia et al., 2021). However, we also observed that the amplitude of spike rate cycles often varied over time, potentially reflecting variability in the strength of these cycles. Such changes in cycle strength could potentially impact seizure features. Second, as with seizure occurrence (Baud et al., 2018; Leguia et al., 2021; Maturana et al., 2020), different cycles likely interact to produce the observed seizure variability. A predictive model incorporating multiple timescales may be more informative than a single spike rate cycle (Panagiotopoulou et al., 2021). Third, we limited our analysis to each patient’s overall spike rate. Spatial patterns of spike rate also vary over time (Chen et al., 2021), and other interictal events such as high frequency activity have different temporal profiles than spike rate (Chen et al., 2021). Spatiotemporal variability in interictal dynamics may be linked to seizure variability (Gliske et al., 2018) and spatial patterns of different interictal events could also be incorporated in multivariate models of seizure features. Finally, although a given state’s occurrence and duration were often independently modulated, there were likely interactions across seizure states. For example, the duration of an early state may depend on whether a seizure progresses to a subsequent possible state (Kaufmann et al., 2020). Approaches such as canonical correlation analysis (Zhuang et al., 2020) could uncover combinations of seizure features that are associated with combinations of interictal features.

Another open question is whether changes in the rate of seizure occurrence are linked to changes in seizure features. In particular, it would be interesting to explore if the timescales associated with seizure occurrence, which we did not examine in our study, also influence seizure evolutions. Many factors could impact both whether seizures occur and seizure features themselves. For example, increasing cortical excitability likely increases seizure likelihood (Meisel et al., 2015) and also facilitates seizure spread (Badawy et al., 2009; Enatsu et al., 2012). However, we also hypothesise that more subtle changes in spatial patterns of cortical excitability could change seizure evolutions without impacting the overall seizure rate. Additional research is needed to determine if there are independent modulators and comodulators of seizure occurrence and seizure evolutions.

Understanding patient-specific seizure variability could provide new clinical strategies for managing seizures in patients with focal epilepsy. First, cycles in seizure variability could be added to seizure forecasting algorithms (Baud and Rao, 2018; Freestone et al., 2017; Stirling et al., 2021), allowing them to forecast not only when a seizure will occur, but also how the seizure will manifest. Thus, seizure forecasting could help anticipate when seizures will be more severe and dangerous to the patient. Additionally, clinicians could modify a patient’s antiepileptic medication based not only on seizures likelihood (Baud and Rao, 2018; Ramgopal et al., 2013; Stirling et al., 2021), but also seizure severity (Cramer and French, 2001). Both interictal and seizure variability may also have implications for treatment efficacy; for example, in a mouse model of temporal lobe epilepsy, optogenetic stimulation only impacted seizures that arose from specific brain states (Ewell et al., 2015). Novel, seizure-specific treatments could therefore be designed to fluctuate over the same timescales as the patient’s seizures, thus delivering time-adaptive treatments that account for the patient’s seizure variability. Finally, uncovering the time-varying mechanisms that underlie seizure variability and severity could provide new targets for manipulating seizures and lessening their impact on patients. As a preliminary step towards clinical applications, future work could connect seizure network states to clinically relevant features, such as onset locations and secondary generalisation. Additionally, repeating our analysis in a larger cohort could determine if certain characteristic temporal patterns of variability, analogous to chronotypes in seizure occurrence (Langdon-Down and Brain, 1929; Leguia et al., 2021; Loddenkemper et al., 2011; Rao et al., 2020), exist across patients.

In summary, we have shown that features of seizure evolutions vary over multiple timescales within individual patients with focal epilepsy. Like interictal dynamics, seizures can change over the course of chronic iEEG recordings as well as over faster timescales, such as circadian and multidien cycles. As with cycles in seizure occurrence, cycles in seizure features can be extracted using interictal spike rate as a biomarker. Future work could explore whether fluctuations in other interictal features, such as spatial patterns of spikes and high frequency activity, explain additional seizure features. Uncovering the timescales of within-patient seizure variability could lead to new approaches for managing and controlling seizures.

5 Methods

5.1 Patients and seizure data

We analysed seizure data from 10 NeuroVista patients that underwent chronic iEEG recordings (Cook et al., 2013). This data has been previously made available by Karoly et al. (2018b). Data from patients NeuroVista 2 and NeuroVista 4 was excluded from our analysis due to low numbers of recorded seizures (32 and 22 seizures, respectively). All other patients had at least 57 analysable seizures. The patients and collection of their chronic iEEG data is described in detail in Cook et al. (2013). Patient details are provided in Supplementary Table S1.1.

Seizures were annotated by clinical staff after identification using patient diaries, audio recordings, and a seizure detection algorithm (Cook et al., 2016). Seizures with clinical manifestations and corresponding iEEG changes (“type 1” seizures) and seizures with iEEG changes comparable to type 1 seizures, but without confirmed clinical manifestations (“type 2” seizures) were included in the analysis (Cook et al., 2016; Karoly et al., 2018b). We excluded seizures with noisy segments (identified visually) and durations of less than 10s.

5.2 Seizure iEEG preprocessing

NeuroVista seizure data was previously notch filtered at 50 Hz during the iEEG acquisition and then bandpass filtered (2nd order, zero-phase Butterworth filter from 1-180 Hz) by Karoly et al. (2018b). After removing any electrodes with noisy or intermittent signal from the analysis, we re-referenced all iEEG to a common average reference. Time periods with signal dropouts were detected using line length and marked as missing data as in Schroeder et al. (2021) (See Supplementary section S7). Section 5.3 describes how this missing data was handled when the seizure time-varying functional connectivity was calculated.

5.3 Computing seizure time-varying functional connectivity

Seizure functional connectivity was defined as band-averaged coherence in six frequency bands: delta 1-4 Hz, theta 4-8 Hz, alpha 8-13 Hz, beta 13-30 Hz, gamma 30-80 Hz, high gamma 80-150

Hz. The time-varying coherence in each frequency band was computed for each seizure from onset to termination using a sliding window (10s window, 9s overlap) as in Schroeder et al. (2020). For each 10s window, the band-averaged coherence was calculated using Welch’s method (2s window, 1s overlap). To tolerate some missing data in each seizure, we allowed functional connectivity in each 10s window to be estimated using a subset of the 2s Welch subwindows. If a 10s time window had five or more 2s subwindows that contained missing data, the seizure was removed from the analysis.

The upper-triangular elements of each symmetric coherence matrix were re-expressed as vectors of length $(n^2 - n)/2$, where n is the number of iEEG channels, and each vector was normalised to have an $L1$ norm of 1. Seizure time windows therefore had $6 \times (n^2 - n)/2$ features describing the pairwise channel interactions in the six different frequency bands.

5.4 Computing progressions of seizure network states

To extract seizure states, patterns of recurring functional connectivity were identified in each patient by applying stability non-negative matrix factorisation (NMF) (Lee and Seung, 1999; Wu et al., 2016) to all of a patient’s seizure functional connectivity time windows using the same pipeline as in our previous work (Schroeder et al., 2020). This step described each patient’s time-varying seizure functional connectivity using (1) a small number of patient-specific NMF basis vectors that captured patterns of functional connectivity, and (2) time-varying coefficients that denoted the contribution of each basis vector to each time window’s connectivity.

We observed that most seizure time windows had a single NMF basis vector with a high coefficient. As such, a time window’s dominant basis vector (i.e., the basis vector with the highest coefficient) provided a simplified description of the time window’s functional connectivity. Therefore, a seizure’s time-varying functional connectivity could be simplified as a sequence, or progression, of network states, where the network state of each time window was the dominant NMF basis vector. We used this approach to describe each patient’s seizures as progressions of network states.

5.5 Preprocessing of interictal spike rate

Detection of interictal epileptiform spikes for this dataset was previously performed and validated (Karoly et al., 2016). The time-varying spike rate for each patient’s recording was summarised as the number of spikes, across all channels, in non-overlapping one hour windows. Due to communication dropouts or failures to regularly store the iEEG data, each one hour segment could have missing segments that affected the spike rate count. To normalise for these dropouts, we normalised each hourly spike rate count by the proportion of captured iEEG data:

$$S_{t,norm} = \frac{S_{t,rec}}{1-D_t}$$

where $S_{t,rec}$ is the recorded spike rate (spikes/hr) of hour t , $S_{t,norm}$ is the spike rate (spikes/hr) of hour t after normalising for dropouts, and D_t is the proportion of dropout time, or missing data, of hour t . Recording hours with $D \geq 0.75$ were considered missing data.

After normalising for dropouts, each hourly spike rate $SR_{t,norm}$ was log transformed:

$$S_t = \log_{10}(S_{t,norm} + 1)$$

yielding the final spike rate, S_t , of each hour t .

Beginning with the shortest missing segments of spike rate data, we then iteratively imputed missing segments of spike rate data using a method similar to Baud et al. (2018). For each missing segment, we first selected the spike rate data segments directly preceding and following the missing segment that were the same length as the missing segment. If this data was available (i.e., did not contain missing values or exceed the endpoints of the recording), we used the surrounding segments to generate spike rate data for the missing segment. This data was generated by linearly interpolating between the means of the surrounding segments and then adding Gaussian noise with a mean of zero and standard deviation of the surrounding segments. Any resulting interpolated data with a spike rate of less than zero was changed to zero. The length of each interpolated segment was also recorded so that interpolated data was only included in the analysis when its length was much shorter ($\leq 20\%$) than the period of the analysed spike rate cycle (extracted in Methods section 5.6). Any remaining missing time points were temporarily set to the mean spike

rate value prior to EMD and then returned to missing values after the decomposition and Hilbert transform (Methods section 5.6).

5.6 Extracting interictal spike rate cycles using EMD

EMD (Huang et al., 1998) was then used to extract modes (referred to as “spike rate cycles” in the Results) from each spike rate time series. Briefly, EMD, decomposes any given signal into a set of signals (called intrinsic mode functions, or IMFs, or “spike rate cycles” in our case) that reconstruct the original signal exactly when summed together (with a residual signal). A key property of each IMF is that it must have approximately the same number (up to ± 1) of extrema as zero-crossings, which ensures that there are no riding waves in the extracted IMFs, as well as a local mean (i.e., the mean of the maximal and minimal envelopes of the IMF) of zero. This property also ensures a well-defined Hilbert transform, e.g. to extract the phase of the signal fluctuations.

We used a variation of EMD known as complete ensemble empirical mode decomposition with adaptive noise (CEEMDAN) (Colominas et al., 2014) that helps ensure that each IMF contains oscillations with a similar timescale (i.e., the mode’s period does not dramatically vary over time) by adding noise to the time series prior to the decomposition. The standard deviation of the added noise was scanned from 0.0025 to 0.125 in steps of 0.0025, and the decomposition at each noise level was performed with 100 noise realisations, a maximum of 1000 sifting iterations to extract each mode, and the signal-to-noise ratio increasing for every stage of the decomposition. This initial step yielded 50 versions, one for each noise level, of the EMD decomposition for each patient’s spike rate time series.

For each decomposition, we used the Hilbert transform to determine the time-varying frequency, phase, and amplitude of each extracted spike rate IMF (Huang et al., 1998). We initially estimated the average period of each IMF using the median frequency of only the original (i.e., non-interpolated) spike rate data, excluding the first and last ten days of the recording due to possible instability in the frequency estimate at the time series boundaries. For each IMF, segments with interpolated spike rate were removed if their duration exceeded 20% of the IMF’s period. To

define each IMF’s timescale, we then recomputed the average period of each IMF as above, now using all of the IMF’s non-missing data. The average amplitude of each IMF was computed using the same process.

For each noise level, we then computed the pairwise index of orthogonality, O (Huang et al., 1998), between all pairs of time series from the EMD decomposition (i.e., the IMFs and the residue signal):

$$O_{i,j} = \frac{1}{T} \sum_{t=1}^T \frac{C_i(t)C_j(t)}{C_i(t)^2 + C_j(t)^2}$$

where $C_i(t)$ is the i th extracted time series, $C_j(t)$ is the j th extracted time series, t is the time point in each time series, and T is the total number of time points with spike rate data in both time series. The normalisation by $\frac{1}{T}$ allowed us to compare O across pairs of time series that had different amounts of missing data due to the spike rate interpolation step. O is close to zero when the two time series are locally orthogonal (i.e., do not contain oscillations at similar frequencies during the same time interval). Thus, to minimise overlap in the frequencies of different spike rate cycles, we found the maximum absolute value of the pairwise O for each decomposition and then selected the noise level that minimised this value. This decomposition was used for all downstream analysis.

The median amplitudes versus median periods of the IMFs of the selected decompositions are shown in S3. To focus our analysis on the primary, robust contributors to spike rate cycles, we limited our analysis to IMFs with locally prominent amplitudes that had median periods that were less than a quarter of the duration of the patient’s recording (see S3). Across patients, we observed a clear distinction between cycles with median periods of approximately one day (0.83 to 1.03 days) and cycles with longer periods (3.93 to 54.77 days). We labeled these timescales as circadian and multidien (i.e., multi-day) cycles, respectively.

5.7 Comparing seizure state occurrence and seizure time since implantation

Most seizure states did not occur in all of a patient’s seizures (Fig. 1E); thus, these states had variable occurrence. For each patient and each of their seizure states with variable occurrence, a

Wilcoxon rank sum test was used to compare the seizure times (i.e., the number of days after the recording’s start that the seizure occurred) of seizures with and without the state. To quantify the temporal separation of seizures with and without the state, the area under the curve (AUC) of the receiver operating characteristic curve for distinguishing state occurrence using seizure times was also computed. Note that AUCs are mathematically equivalent to Wilcoxon rank sum tests, and therefore have the same statistical significance as the Wilcoxon rank sum test statistic.

5.8 Comparing seizure state duration and seizure time since implantation

To compare state durations to seizure times in the recording, we computed the Spearman correlation between non-zero state durations and the number of days since the start of the recording that the corresponding seizures occurred. Spearman’s correlation was also computed between the total duration of all seizures and seizure times in the recording.

5.9 Comparing seizure state occurrence and spike rate cycles

For each patient and each of their seizure states with variable occurrence, we determined the IMF (“spike rate cycle”) phases preferences of seizures with the seizure state. For each IMF, a seizure’s phase was defined as the phase of the IMF during the hour in which the seizure occurred, and seizures were excluded from the analysis if this spike rate data was missing. To quantify the phase preference of a given state and IMF, we first computed the mean resultant vector from the IMF phases of all seizures with the state:

$$Re^{-i\psi} = \frac{1}{S} \sum_{s=1}^S e^{-i\phi_s}$$

Here, S is the number of seizures containing the state, s is a seizure with the state, ϕ_s is the IMF phase of seizure s , R is the modulus of the mean resultant vector, and ψ is the angle of the mean resultant vector. As in previous work (Baud et al., 2018; Leguia et al., 2021), we refer to R as the PLV of seizures containing the state. The PLV varies from 0 to 1 and is higher when the IMF phases are similar across all seizures with the state.

To control for any seizure phase preference, we used permutation tests to determine the significance of the observed PLV for each seizure state and IMF (“spike rate cycle”). For a state that occurred S times, we randomly selected S seizures from all analysed seizures and recomputed the PLV. Repeating this process for 10,000 different permutations yielded a null distribution of PLV if the seizure state had no additional phase preference within that spike rate cycle. The p -value of the association was defined as the percentage of times a permuted PLV was greater than or equal to the observed PLV.

5.10 Comparing seizure state duration and spike rate cycles

For each patient, we also compared the durations of each seizure state to the patient’s spike rate cycles. For each IMF (“spike rate cycle”) and state, we found the IMF phases of seizures that contained the state and computed the rank linear-circular correlation D between the state’s duration and the IMF phases (Mardia, 1976). D varies from 0 to 1, with higher values indicating a stronger association between the state’s duration and the IMF phases. We determined the significance of these associations by permuting these state durations 10,000 times and computing a null distribution of correlations. The p -value of the observed correlation was the percentage of times a permuted correlation was greater than or equal to the observed correlation. We used the same approach to compare each patient’s overall seizure durations to each spike rate cycle.

5.11 Comparing spike rate and seizure states

We also compared the overall spike rate, prior to EMD, to state occurrences and state durations using Wilcoxon rank sum tests and Spearman’s correlation, respectively (Supplementary section S5).

5.12 Correction for multiple comparisons

Benjamini-Hochberg FDR correction for multiple comparisons, with $\alpha = 0.05$, was performed for all tests across all patients that compared seizure features (state occurrence, state duration, and

seizure duration) to temporal features (seizure time in the recording, spike rate cycles, and overall spike rate). Uncorrected p -values are reported in the text.

5.13 Code and data availability

All analysis was performed in MATLAB version R2018b. CEEMDAN of interictal spike rate was performed using the MATLAB package CEEMDAN (<https://github.com/macolominas/CEEMDAN>) (Colominas et al., 2014; Torres et al., 2011). The remaining analysis was performed using custom MATLAB scripts. The NeuroVista seizure iEEG data used in this study is available from www.epilepsyecosystem.org. The processed data (NMF W and H matrices) and seizure durations of all subjects, along with analysis code is available on Zenodo (DOI 10.5281/zenodo.5503590).

5.14 Acknowledgements

We thank members of the Computational Neurology, Neuroscience & Psychiatry Lab (www.cnnp-lab.com) for discussions on the analysis and manuscript; P.N.T. and Y.W. are both supported by UKRI Future Leaders Fellowships (MR/T04294X/1, MR/V026569/1).

Supplementary

S1 Patient metadata

Table S1.1 provides the following metadata for the NeuroVista patients:

- **Age (yrs):** patient age in years.
- **Sex:** patient sex.
- **Age at diagnosis (yrs):** patient age when they were diagnosed with epilepsy, in years.
- **Lobe:** purported lobe of onset of the patient’s seizures, based on clinical findings. Note that some patients had seizures arising from multiple lobes (e.g., OP = occipital/parietal onset).
- **Previous resection:** whether the patient had undergone surgical resection prior to the chronic recording.
- **# seizures analysed:** number of the patient’s seizures analysed in this work.
- **# electrodes analysed:** number of recording electrodes included in the analysis after removing noisy electrodes.
- **Total recording time (days):** total duration of the intracranial recording time, in days.
- **Sampling frequency:** sampling frequency at which intracranial data was acquired and stored.

Subject	Age (yrs)	Sex	Age at diagnosis (yrs)	Lobe	Previous resection	# of seizures analysed	# of electrodes analysed	Total recording time (days)	Sampling frequency
NeuroVista 1	26	M	4	PT	No	94	15	767.4	400 Hz
NeuroVista 3	22	F	16	PT	Yes	273	16	557.5	400 Hz
NeuroVista 6	62	M	37	T	No	69	16	441.3	400 Hz
NeuroVista 7	52	M	26	FT	No	212	16	184.8	400 Hz
NeuroVista 8	48	M	20	FT	Yes	452	14	558.4	400 Hz
NeuroVista 9	51	F	10	OP	No	147	14	394.9	400 Hz
NeuroVista 10	50	F	15	FT	Yes	446	16	373.2	400 Hz
NeuroVista 11	53	F	15	FT	No	351	14	721.6	400 Hz
NeuroVista 13	50	M	20	T	Yes	425	16	746.9	400 Hz
NeuroVista 15	36	M	5	T	Yes	57	16	465.6	400 Hz

Sex
M = male, F = female

Lobe
T = temporal, F = frontal,
P = parietal, O = occipital,
IH = interhemispheric

Table S1.1: Metadata of NeuroVista patients. Clinical metadata and patient demographics are reproduced from Cook et al. (2013).

S2 Seizure network states of an example patient, NeuroVista 1

Fig. S2.1 shows the six network states of NeuroVista 1. Each state was derived using stability NMF (Wu et al., 2016), as in Schroeder et al. (2020).

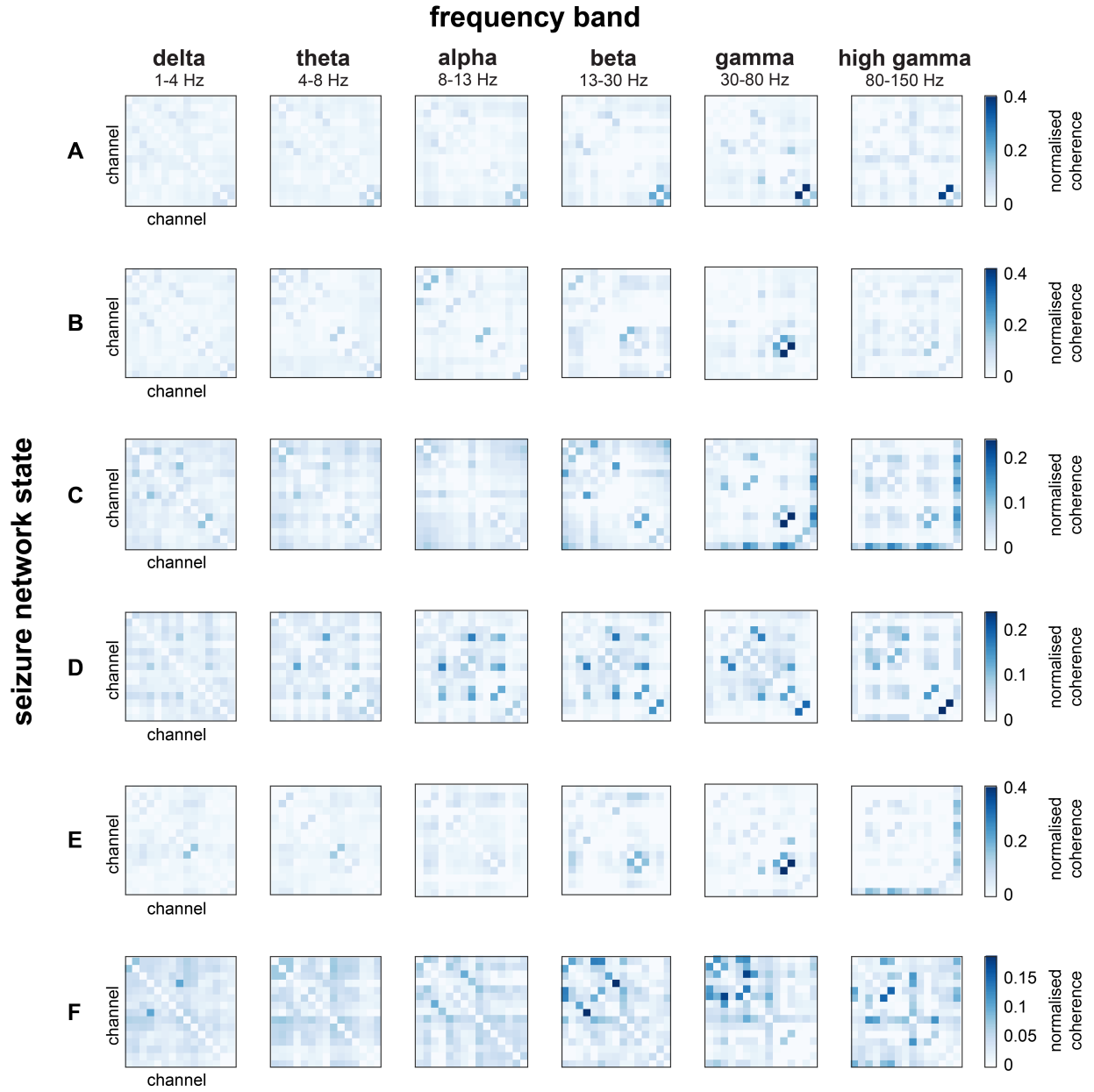


Figure S2.1: Seizure network states of NeuroVista 1. Rows correspond to seizure network states. Each network state describes the coherence between pairs of iEEG channels in six frequency bands (columns). Thus, each network state is composed of six functional connectivity matrices, one for each frequency band. Each matrix is normalised so that the upper triangular elements sum to one. Colormap limits are consistent within each state (i.e., across each row). Self-connections (diagonal matrix elements) are not shown.

S3 EMD of interictal spike rate and selection of spike rate cycles for comparison with seizure features

For each patient, we used EMD to extract cycles in interictal spike rate. Fig. S3.1 shows the median amplitudes versus median periods (days/cycle) of each EMD cycle. We limited our analysis to cycles that had both (1) locally prominent amplitudes, which we defined as local maxima (found using MATLAB function *findpeaks*) in these plots with amplitudes greater than or equal to 20% of the patient's highest median IMF amplitude and (2) median periods of less than a quarter of the recording's duration. These cycles are shown using the coloured circles in each patient. The fastest IMF of each patient was not included in the analysis since these oscillations are often thought to contain temporally unstructured noise.

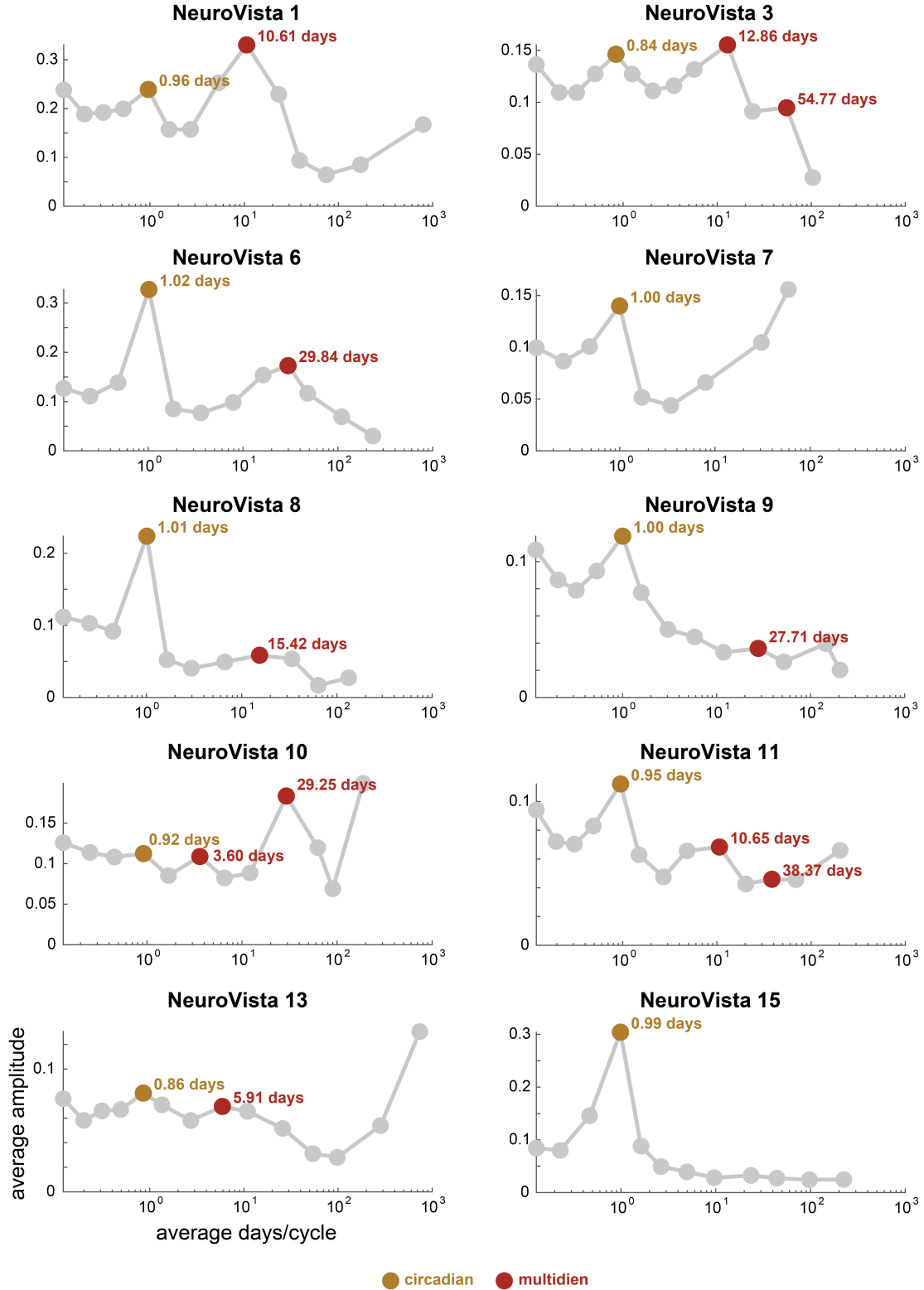


Figure S3.1: Amplitudes and periods of the spike rate cycles extracted using EMD. Each plot shows the median amplitude and period of all of the extracted spike rate cycles (circles) of each patient. Coloured circles indicate cycles that were analysed in this study, with the colour indicating the timescale category of the cycle (circadian or multidien). Spike rate residues are not shown.

S4 First and last occurrences of seizure states in patient recordings

Fig. S4.1 shows the first and last known occurrences of each seizure state in each patient. Each state visualisation is also coloured by whether the state's occurrence was significantly associated with the time since the start of the recording. As a reminder, states are patient-specific, even if they share the same letter label. In most cases, the time from first to last occurrence of a seizure state spans the majority of the patient's recording. Thus, most states are not limited to a specific section of the recording.

Note that due to missing and noisy data, some of the patient's seizures were not captured in the iEEG recordings. As such, some states may have occurred earlier or later in the recording period than displayed here. As such, this analysis can only conclusively say when seizure states *did* occur, and there is some uncertainty regarding when states *did not* occur.

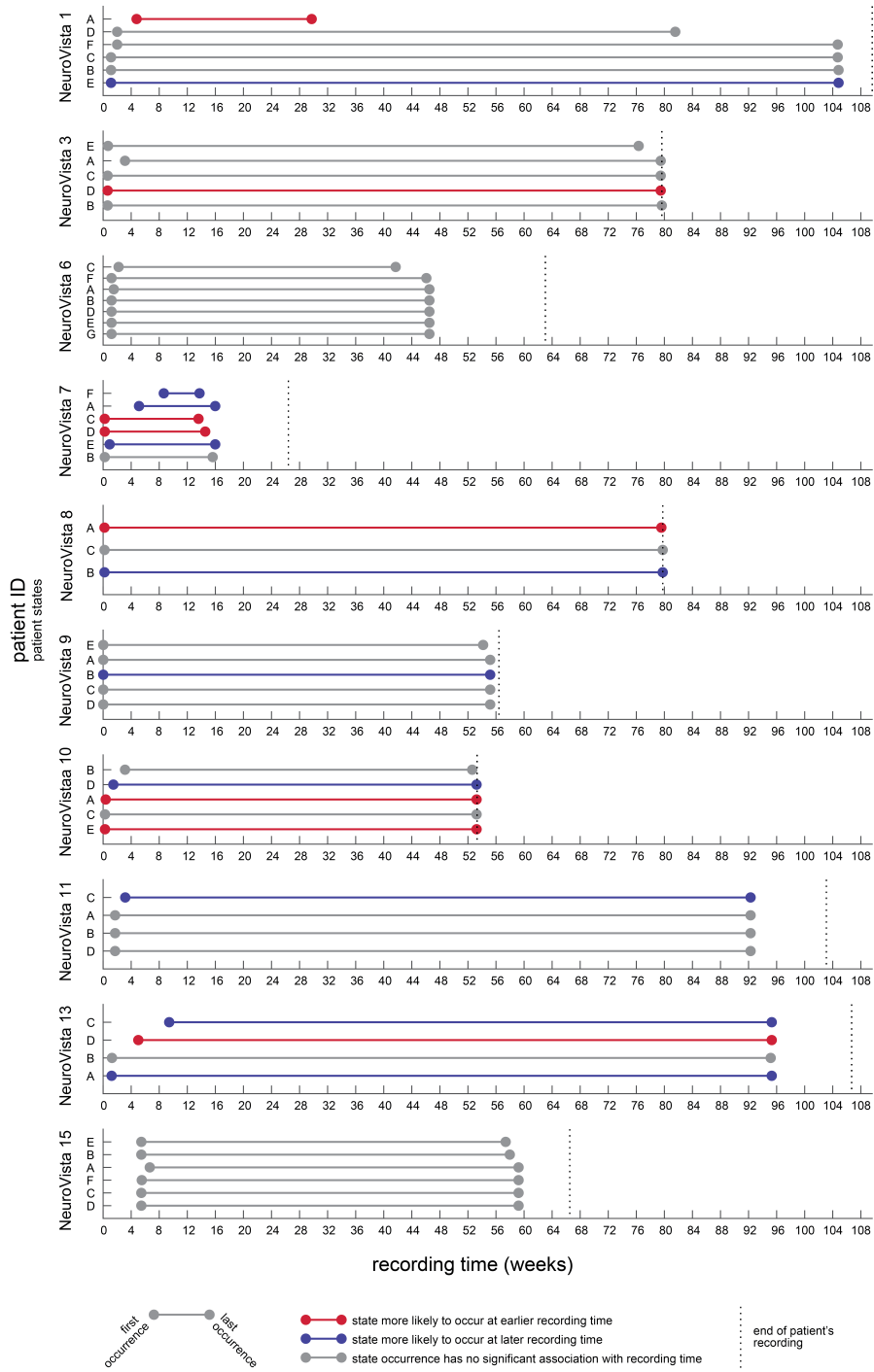


Figure S4.1: First and last known occurrences of each seizure state in each patient. In each patient, the times in the recording of the first and last occurrences of each seizure state (circles), with the time spanned by those occurrence marked with horizontal line. States are ordered from the shortest to longest amount of time that they spanned. State markers are coloured by whether the state's occurrence was significantly associated with the time since implantation.

S5 Supplementary spike rate, seizure duration, and seizure state analyses and visualisations

Fig. S5.1 shows which seizure state and total seizure duration were significantly associated with seizure time since implantation, spike rate cycles, and spike rate in each patient. We emphasise that states are *not* comparable across patients, even if they share the same label and colour.

The first columns in Fig. S5.1A and S5.1B show which states were significantly associated with overall spike rate after FDR correction for multiple comparisons. While overall spike rate was often associated with these seizure features, it was usually associated with the same or fewer states than specific timescales (spike rate cycles and time since implantation) (Fig. S5.1). The only exceptions were the occurrence of state C in NeuroVista 1, the durations of states C and D in NeuroVista 6 and, the duration of state C in NeuroVista 10, which were only associated with overall spike rate. Cases where overall spike rate, but not individual spike rate fluctuations, are associated with states may be due to spike rate features that our analysis did not capture (e.g., cycle amplitude) or joint effects of modulations over different timescales that were not significant at the level of individual timescales.

Fig. S5.1B also indicates when a patient's total seizure duration was associated with overall spike rate, spike rate cycles, and/or recording time. Seizure duration was only associated with spike rate cycles in two patients and recording time in four patients; thus, state duration associations were more widespread than seizure duration associations in our cohort.

A. State occurrence



B. State duration

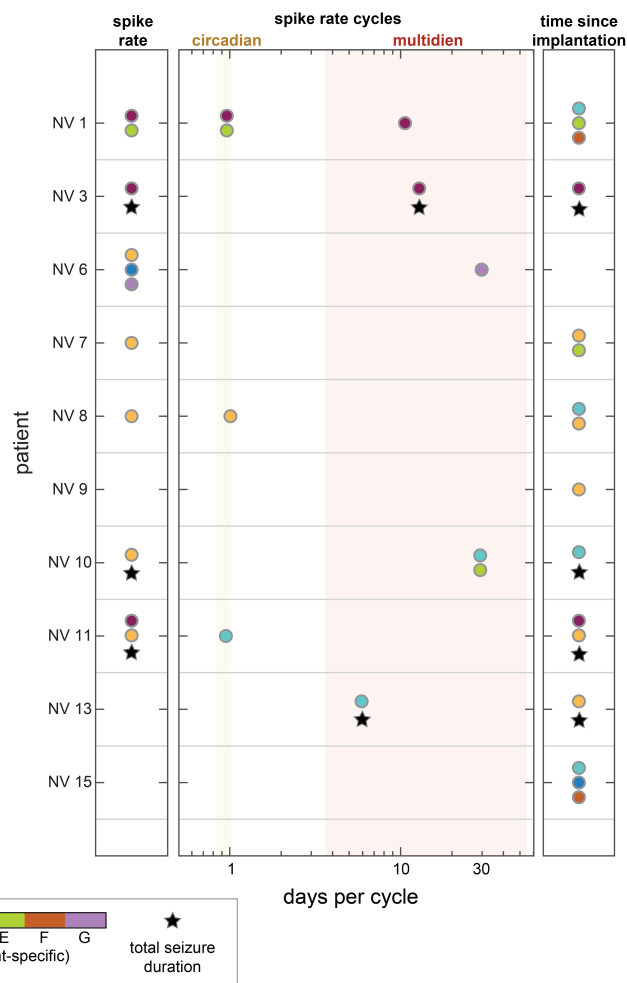


Figure S5.1: Seizure states significantly associated with recording time, spike rate cycles, and spike rate. Coloured circles indicate the seizure states with occurrences (A) or state duration (B) were significantly associated with overall spike rate (left columns), spike rate cycles (middle columns), and recording time (right columns). Rows for different patients are demarcated by horizontal grey lines. States are not comparable across patients, but are comparable within each patient. In (B), associations with total seizure duration are also marked with a black star.

S6 Locations of modulated states in seizure network state evolutions

We also investigated whether modulated states tended to occur during certain parts of seizure evolutions. In each patient, we first identified the order in which states occurred in each seizure. Only the first occurrence of a state was considered; for example, in the hypothetical seizure state progression

BBBAAACCACCCEEEEE

state *B* would be first, *A* would be second, *C* would be third, and *E* would be fourth. This seizure does not provide any information about other states, such as state *D*. A state's *location* was then defined as the state's most common (i.e., mode) order of occurrence across all the patient's seizures that included the state. Fig. S6.1A shows the distributions of state locations in each patient. Across all patients, we then computed the mean state location for four categories of states (Fig. S6.1B, top row, left to right): (1) states whose occurrence was associated with seizure recording time, (2) states whose duration was associated with seizure recording time, (3) states whose occurrence was associated with at least one spike rate cycle, and (4) states whose duration was associated with at least one spike rate cycle.

We then performed permutation tests to determine whether significant states occurred earlier or later in the seizure evolutions than expected by chance (Fig. S6.1B, bottom row). For each scenario, we permuted state labels in each patient, selected the same number of "significant" states and their corresponding locations from each patient, and then recomputed the mean state location across all patients. Thus, this permutation test accounts for the distribution of state locations in each patient. For each test, the null distribution of mean state locations was computed using 10,000 permutations. The *p*-value of the observed mean location was defined as the percentage of permutations with a mean location as extreme (i.e., equidistant from the centre of the distribution) as the observed mean location. In all scenarios, the mean state location did not significantly differ from chance, suggesting that states that occurred earlier or later in seizure evolutions were not preferentially modulated.

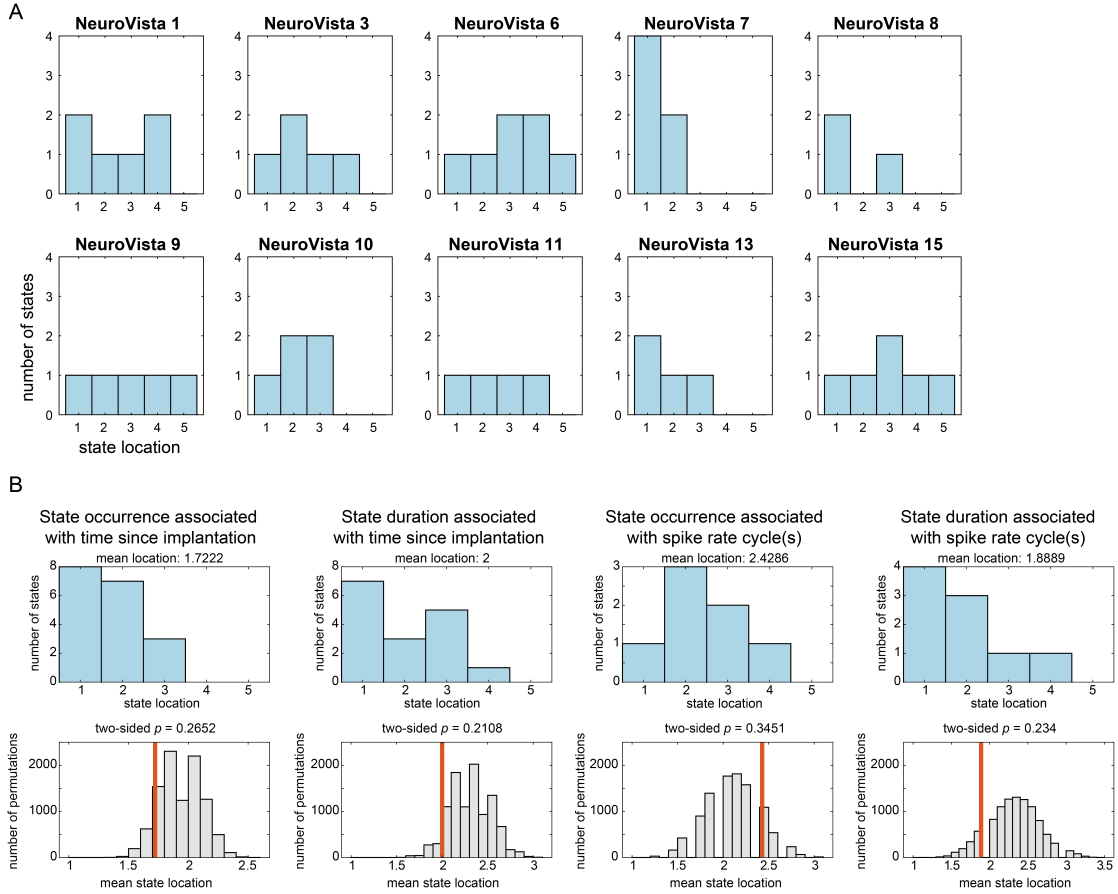


Figure S6.1: Locations of significant seizure states in seizure network state evolutions. A) Distributions of state locations in each patient. B) State locations of states significantly associated with seizure recording time and spike rate cycles. Top row: distributions of locations of significantly associated states. Bottom row: permutation test results for determining the significance of the mean state location in each scenario. The observed mean state location is marked with a red line in each distribution of permuted mean state locations.

S7 Detecting signal dropouts

The NeuroVista data contains time periods of signal dropouts when the iEEG signal was not recorded. We used line length to identify iEEG segments with no signal (i.e., a flat time series with no voltage changes). We defined the line length L of a time series as

$$L = \frac{1}{T-1} \sum_{i=1}^{T-1} |x_{i+1} - x_i|$$

where x_i is the i th time point in a time series with T time points.

The time-varying line length of each seizure was computed for each iEEG channel in sliding windows (1/10s window, 1/20s overlap). Any time windows with 8 or more channels with line length ≤ 0.5 , along with the preceding and following time windows, were considered missing data.

References

- Radwa Badawy, Richard Macdonell, Graeme Jackson, and Samuel Berkovic. The peri-ictal state: Cortical excitability changes within 24 h of a seizure. *Brain*, 132:1013–1021, 2009. ISSN 00068950. doi: 10.1093/brain/awp017.
- Maxime O. Baud and Vikram R. Rao. Gauging seizure risk. *Neurology*, 91:967–973, 2018. ISSN 1526632X. doi: 10.1212/WNL.0000000000006548.
- Maxime O Baud, Jonathan K Kleen, Emily A Mirro, Jason C Andrechak, David King-Stephens, Edward F Chang, and Vikram R Rao. Multi-day rhythms modulate seizure risk in epilepsy. *Nature Communications*, 9(88):1–10, 2018. doi: 10.1038/s41467-017-02577-y.
- C W Bazil. Seizure modulation by sleep and sleep state. *Brain Research*, 1703:13–17, 2018.
- C W Bazil and T S Walczak. Effects of sleep and sleep stage on epileptic and nonepileptic seizures. *Epilepsia*, 38(1):56–62, 1997. ISSN 0013-9580. doi: 10.1111/j.1528-1157.1997.tb01077.x.
- Samuel P Burns, Sabato Santaniello, Robert B Yaffe, Christophe C Jouny, Nathan E Crone, Gregory K Bergey, William S Anderson, and Sridevi V Sarma. Network dynamics of the brain and influence of the epileptic seizure onset zone. *Proceedings of the National Academy of Sciences*, 111(49):E5321–E5330, 2014. doi: 10.1073/pnas.1401752111.
- Zhuying Chen, David B. Grayden, Anthony N. Burkitt, Udaya Seneviratne, Wendyl J. D’Souza, Chris French, Philippa J. Karoly, Katrina Dell, Kent Leyde, Mark J. Cook, and Matias I. Maturana. Spatiotemporal Patterns of High-Frequency Activity (80-170 Hz) in Long-Term Intracranial EEG. *Neurology*, 96(7):e1070–e1081, 2021. ISSN 1526632X. doi: 10.1212/WNL.0000000000011408.
- Marcelo A. Colominas, Gastón Schlotthauer, and María E. Torres. Improved complete ensemble EMD: A suitable tool for biomedical signal processing. *Biomedical Signal Processing and Control*, 14:19–29, 2014. ISSN 17468108. doi: 10.1016/j.bspc.2014.06.009.

- Mark J. Cook, Terence J. O'Brien, Samuel F. Berkovic, Michael Murphy, Andrew Morokoff, Gavin Fabinyi, Wendyl D'Souza, Raju Yerra, John Archer, Lucas Litewka, Sean Hosking, Paul Lightfoot, Vanessa Ruedebusch, W. Douglas Sheffield, David Snyder, Kent Leyde, and David Himes. Prediction of seizure likelihood with a long-term, implanted seizure advisory system in patients with drug-resistant epilepsy: A first-in-man study. *The Lancet Neurology*, 12:563–571, 2013. ISSN 14744422. doi: 10.1016/S1474-4422(13)70075-9.
- Mark J. Cook, Philippa J. Karoly, Dean R. Freestone, David Himes, Kent Leyde, Samuel Berkovic, Terence O'Brien, David B. Grayden, and Ray Boston. Human focal seizures are characterized by populations of fixed duration and interval. *Epilepsia*, 57(3):359–368, 2016. ISSN 15281167. doi: 10.1111/epi.13291.
- Joyce A. Cramer and Jacqueline French. Quantitative assessment of seizure severity for clinical trials: A review of approaches to seizure components. *Epilepsia*, 42(1):119–129, 2001. ISSN 00139580. doi: 10.1046/j.1528-1157.2001.19400.x.
- Kathryn A. Davis, Beverly K. Sturges, Charles H. Vite, Vanessa Ruedebusch, Gregory Worrell, Andrew B. Gardner, Kent Leyde, W. Douglas Sheffield, and Brian Litt. A novel implanted device to wirelessly record and analyze continuous intracranial canine eeg. *Epilepsy Research*, 96(1):116–122, 2011. ISSN 0920-1211. doi: <https://doi.org/10.1016/j.eplepsyres.2011.05.011>.
- Rei Enatsu, Kazutaka Jin, Sherif Elwan, Yuichi Kubota, Zhe Piao, Timothy O'Connor, Karl Horning, Richard C. Burgess, William Bingaman, and Dileep R. Nair. Correlations between ictal propagation and response to electrical cortical stimulation: A cortico-cortical evoked potential study. *Epilepsy Research*, 101:76–87, 2012. ISSN 09201211. doi: 10.1016/j.eplepsyres.2012.03.004.
- Laura A. Ewell, Liang Liang, Caren Armstrong, Ivan Soltész, Stefan Leutgeb, and Jill K. Leutgeb. Brain state is a major factor in preseizure hippocampal network activity and influences success of seizure intervention. *The Journal of Neuroscience*, 35(47):15635–15648, 2015. ISSN 0270-6474. doi: 10.1523/JNEUROSCI.5112-14.2015.

- Dean R. Freestone, Philippa J. Karoly, and Mark J. Cook. A forward-looking review of seizure prediction. *Current Opinion in Neurology*, 30:167–173, 2017. ISSN 1350-7540. doi: 10.1097/WCO.0000000000000429.
- Stephen V. Gliske, Zachary T. Irwin, Cynthia Chestek, Garnett L. Hegeman, Benjamin Brinkmann, Oren Sagher, Hugh J. L. Garton, Greg A. Worrell, and William C. Stacey. Variability in the location of high frequency oscillations during prolonged intracranial EEG recordings. *Nature Communications*, 9:2155, 2018. ISSN 2041-1723. doi: 10.1038/s41467-018-04549-2.
- W. R. Gowers. *Epilepsy and other chronic convulsive diseases: their causes, symptoms, and treatment*. William Wood & Company, New York, 1885.
- J. Jeffry Howbert, Edward E. Patterson, S. Matt Stead, Ben Brinkmann, Vincent Vasoli, Daniel Crepeau, Charles H. Vite, Beverly Sturges, Vanessa Ruedebusch, Jaideep Mavoori, Kent Leyde, W. Douglas Sheffield, Brian Litt, and Gregory A. Worrell. Forecasting seizures in dogs with naturally occurring epilepsy. *PLoS ONE*, 9(1):e81920, 2014. ISSN 19326203. doi: 10.1371/journal.pone.0081920.
- David Hsu, Wei Chen, Murielle Hsu, and John M. Beggs. An open hypothesis: Is epilepsy learned, and can it be unlearned? *Epilepsy and Behavior*, 13:511–522, 2008. ISSN 15255050. doi: 10.1016/j.yebeh.2008.05.007.
- Norden E Huang, Zheng Shen, Steven R Long, Manli C Wu, Hsing H. Shih, Quanan Zheng, Nai Chyuan Yen, Chi Chao Tung, and Henry H Liu. The empirical mode decomposition and the Hubert spectrum for nonlinear and non-stationary time series analysis. *Proceedings of the Royal Society A: Mathematical, Physical and Engineering Sciences*, 454:903–995, 1998. ISSN 13645021. doi: 10.1098/rspa.1998.0193.
- D Janz. The grand mal épilepsies and the sleeping-waking cycle. *Epilepsia*, 3(1):69–109, 1962. doi: <https://doi.org/10.1111/j.1528-1157.1962.tb05235.x>.
- Beata Jarosiewicz and Martha Morrell. The RNS system: brain-responsive neurostimulation for

the treatment of epilepsy. *Expert Review of Medical Devices*, 18(2):129–138, 2021. doi: 10.1080/17434440.2019.1683445. PMID: 32936673.

Diego Jiménez-Jiménez, Ramesh Nekkare, Lorena Flores, Katerina Chatzidimou, Istvan Bodi, Mrinalini Honavar, Nandini Mullatti, Robert D C Elwes, Richard P. Selway, Antonio Valentín, and Gonzalo Alarcón. Prognostic value of intracranial seizure onset patterns for surgical outcome of the treatment of epilepsy. *Clinical Neurophysiology*, 126:257–267, 2015. ISSN 18728952. doi: 10.1016/j.clinph.2014.06.005.

Philippa J. Karoly, Dean R. Freestone, Ray Boston, David B. Grayden, David Himes, Kent Leyde, Udaya Seneviratne, Samuel Berkovic, Terence O’Brien, and Mark J. Cook. Interictal spikes and epileptic seizures: Their relationship and underlying rhythmicity. *Brain*, 139:1066–1078, 2016. ISSN 14602156. doi: 10.1093/brain/aww019.

Philippa J. Karoly, Daniel M. Goldenholz, Dean R. Freestone, Robert E. Moss, David B. Grayden, William H. Theodore, and Mark J. Cook. Circadian and circaseptan rhythms in human epilepsy: a retrospective cohort study. *The Lancet Neurology*, 17:977–985, 2018a. ISSN 14744465. doi: 10.1016/S1474-4422(18)30274-6.

Philippa J Karoly, Levin Kuhlmann, Daniel Soudry, David B Grayden, Mark J Cook, and Dean R Freestone. Seizure pathways: a model-based investigation. *PLoS Computational Biology*, 14(10): e1006403, 2018b. doi: 10.26188/5b6a999fa2316.

Philippa J. Karoly, Vikram R. Rao, Nicholas M. Gregg, Gregory A. Worrell, Christophe Bernard, Mark J. Cook, and Maxime O. Baud. Cycles in epilepsy. *Nature Reviews Neurology*, 17(May), 2021. ISSN 17594766. doi: 10.1038/s41582-021-00464-1.

Elisabeth Kaufmann, Magdalena Seethaler, Michael Lauseker, Min Fan, Christian Vollmar, Soheyl Noachtar, and Jan Rémi. Who seizes longest? Impact of clinical and demographic factors. *Epilepsia*, 61:1376–1385, 2020. ISSN 15281167. doi: 10.1111/epi.16577.

Ankit N. Khambhati, Kathryn A. Davis, Brian S. Oommen, Stephanie H. Chen, Timothy H. Lucas, Brian Litt, and Danielle S. Bassett. Dynamic network drivers of seizure generation, propagation

- and termination in human neocortical epilepsy. *PLoS Computational Biology*, 11(12):e1004608, 2015. ISSN 15537358. doi: 10.1371/journal.pcbi.1004608.
- Ankit N. Khambhati, Kathryn A. Davis, Timothy H. Lucas, Brian Litt, and Danielle S. Bassett. Virtual cortical resection reveals push-pull network control preceding seizure evolution. *Neuron*, 91:1170–1182, 2016. ISSN 10974199. doi: 10.1016/j.neuron.2016.07.039.
- David King-Stephens, Emily Mirro, Peter B Weber, Kenneth D Laxer, Paul C Van Ness, Vicenta Salanova, David C Spencer, Christianne N Heck, Alica Goldman, Barbara Jobst, Donald C Shields, Gregory K Bergey, Stephan Eisenschenk, Gregory A Worrell, Marvin A Rossi, Robert E Gross, Andrew J Cole, Michael R Sperling, Dileep R Nair, Ryder P. Gwinn, Yong D Park, Paul A Rutecki, Nathan B Fountain, Robert E Wharen, Lawrence J Hirsch, Ian O Miller, Gregory L Barkley, Jonathan C Edwards, Eric B Geller, Michel J Berg, Toni L Sadler, Felice T Sun, and Martha J Morrell. Lateralization of mesial temporal lobe epilepsy with chronic ambulatory electrocorticography. *Epilepsia*, 56(6):959–967, 2015. doi: 10.1111/epi.13010.
- Marie Therese Kuhnert, Christian E. Elger, and Klaus Lehnertz. Long-term variability of global statistical properties of epileptic brain networks. *Chaos*, 20(043126), 2010. ISSN 10541500. doi: 10.1063/1.3504998.
- Mary Langdon-Down and W. R. Brain. Time of day in relation to convulsions in epilepsy. *Lancet*, 213(5516):1029–1032, 1929.
- D D Lee and H S Seung. Learning the parts of objects by non-negative matrix factorization. *Nature*, 401:788–791, 1999. ISSN 0028-0836. doi: 10.1038/44565.
- Marc G Leguia, Ralph G. Andrzejak, Christian Rummel, Joline M. Fan, Emily A. Mirro, Thomas K. Tcheng, Vikram R. Rao, and Maxime O. Baud. Seizure Cycles in Focal Epilepsy. *JAMA Neurology*, 78(4):454–463, 2021. doi: 10.1001/jamaneurol.2020.5370.
- T. Loddenkemper, M. Vendrame, M. Zarowski, M. Gregas, A. V. Alexopoulos, E. Wyllie, and S. V. Kothare. Circadian patterns of pediatric seizures. *Neurology*, 76:145–153, 2011. ISSN 00283878. doi: 10.1212/WNL.0b013e318206ca46.

- K. V. Mardia. Linear-circular correlation coefficients and rhythmometry. *Biometrika*, 63(2):403–405, 1976.
- Matias I Maturana, Christian Meisel, Katrina Dell, Philippa J Karoly, Wendyl D’Souza, David B Grayden, Anthony N Burkitt, Premysl Jiruska, Jan Kudlacek, Jaroslav Hlinka, Mark J Cook, Levin Kuhlmann, and Dean R Freestone. Critical slowing down as a biomarker for seizure susceptibility. *Nature Communications*, 11:2172, 2020. ISSN 20411723. doi: 10.1038/s41467-020-15908-3.
- Christian Meisel, Andreas Schulze-Bonhage, Dean Freestone, Mark James Cook, Peter Achermann, and Dietmar Plenz. Intrinsic excitability measures track antiepileptic drug action and uncover increasing/decreasing excitability over the wake/sleep cycle. *Proceedings of the National Academy of Sciences*, 112(47):14694–14699, 2015. ISSN 0027-8424. doi: 10.1073/pnas.1513716112.
- Georgios D. Mitsis, Maria N. Anastasiadou, Manolis Christodoulakis, Eleftherios S. Papathanasiou, Savvas S. Papacostas, and Avgis Hadjipapas. Functional brain networks of patients with epilepsy exhibit pronounced multiscale periodicities, which correlate with seizure onset. *Human Brain Mapping*, 41:2059–2076, 2020. ISSN 10970193. doi: 10.1002/hbm.24930.
- Jason S. Naftulin, Omar J. Ahmed, Giovanni Piantoni, Jean Baptiste Eichenlaub, Louis Emmanuel Martinet, Mark A. Kramer, and Sydney S. Cash. Ictal and preictal power changes outside of the seizure focus correlate with seizure generalization. *Epilepsia*, 59:1398–1409, 2018. ISSN 15281167. doi: 10.1111/epi.14449.
- Cayetano E. Napolitano and Miguel A. Orriols. Changing patterns of propagation in a super-refractory status of the temporal lobe. Over 900 seizures recorded over nearly one year. *Epilepsy and Behavior Case Reports*, 1:126–131, 2013. ISSN 22133232. doi: 10.1016/j.ebcr.2013.07.001.
- Allison Navis and Cynthia Harden. A Treatment Approach to Catamenial Epilepsy. *Current Treatment Options in Neurology*, 18:30, 2016. ISSN 15343138. doi: 10.1007/s11940-016-0413-6.
- Soheyl Noachtar and Astrid S. Peters. Semiology of epileptic seizures: A critical review. *Epilepsy and Behavior*, 15:2–9, 2009. ISSN 15255050. doi: 10.1016/j.yebeh.2009.02.029.

- Mariella Panagiotopoulou, Christoforos Papasavvas, Gabrielle M Schroeder, Peter Taylor, and Yujiang Wang. Fluctuations in eeg band power at subject-specific timescales over minutes to days are associated with changes in seizure dynamics. *arXiv*, q-bio.NC:2012.07105, 2021.
- Frederick L. Patry. The relation of time of day, sleep, and other factors to the incidence of epileptic seizures. *American Journal of Psychiatry*, 87(5):789–813, 1931. doi: 10.1176/ajp.87.5.789.
- Sriram Ramgopal, Sigride Thome-Souza, and Tobias Loddenkemper. Chronopharmacology of Anti-Convulsive Therapy. *Current Neurology and Neuroscience Reports*, 13:339, mar 2013. ISSN 1534-6293. doi: 10.1007/s11910-013-0339-2.
- Vikram R. Rao, Marc G. Leguia, Thomas K. Tcheng, and Maxime O. Baud. Cues for seizure timing. *Epilepsia*, 62(S1):S15–S31, 2020. ISSN 15281167. doi: 10.1111/epi.16611.
- M Ryzi, M Brazdil, Z Novak, J Hemza, J Chrastina, H Oslejskova, I Rektor, and R Kuba. Long-term outcomes in patients after epilepsy surgery failure. *Epilepsy Research*, 110:71–77, 2015. ISSN 1872-6844.
- Maria Luisa Saggio, Dakota Crisp, Jared Scott, Phillippa J Karoly, Levin Kuhlmann, Mitsuyoshi Nakatani, Tomohiko Murai, Matthias Dümpelmann, Andreas Schulze-Bonhage, Akio Ikeda, Mark Cook, Stephen V Gliske, Jack Lin, Christophe Bernard, Viktor Jirsa, and William Stacey. A taxonomy of seizure dynamotypes. *Elife*, 9:e55632, 2020. doi: <https://doi.org/10.7554/eLife.55632>.
- Pariya Salami, Noam Peled, Jessica K. Nadalin, Louis Emmanuel Martinet, Mark A. Kramer, Jong W. Lee, and Sydney S. Cash. Seizure onset location shapes dynamics of initiation. *Clinical Neurophysiology*, 131:1782–1797, 2020. ISSN 18728952. doi: 10.1016/j.clinph.2020.04.168.
- Gabrielle M. Schroeder, Beate Diehl, Fahmida A. Chowdhury, John S. Duncan, Jane de Tisi, Andrew J. Trevelyan, Rob Forsyth, Andrew Jackson, Peter N. Taylor, and Yujiang Wang. Seizure pathways change on circadian and slower timescales in individual patients with focal epilepsy. *Proceedings of the National Academy of Sciences*, 117(20):11048–11058, 2020. ISSN 0027-8424. doi: 10.1073/pnas.1922084117.

- Gabrielle M. Schroeder, Fahmida A. Chowdhury, Mark J. Cook, Beate Diehl, John S. Duncan, Philippa J. Karoly, Peter N. Taylor, and Yujiang Wang. Seizure pathways and seizure durations can vary independently within individual patients with focal epilepsy, 2021.
- S. Sinha, M. Brady, C. A. Scott, and M. C. Walker. Do seizures in patients with refractory epilepsy vary between wakefulness and sleep? *Journal of Neurology, Neurosurgery and Psychiatry*, 77: 1076–1078, 2006. ISSN 00223050. doi: 10.1136/jnnp.2006.088385.
- Rachel E. Stirling, Mark J. Cook, David B. Grayden, and Philippa J. Karoly. Seizure forecasting and cyclic control of seizures. *Epilepsia*, 62(S1):S2–S14, 2021. ISSN 15281167. doi: 10.1111/epi.16541.
- María E. Torres, Marcelo A. Colominas, Gastón Schlotthauer, and Patrick Flandrin. A complete ensemble empirical mode decomposition with adaptive noise. In *2011 IEEE International Conference on Acoustics, Speech and Signal Processing (ICASSP)*, pages 4144–4147, 2011. doi: 10.1109/ICASSP.2011.5947265.
- Hoameng Ung, Kathryn A Davis, Drausin Wulsin, Joost Wagenaar, Emily Fox, John J McDonnell, Ned Patterson, Charles H Vite, Gregory Worrell, and Brian Litt. Temporal behavior of seizures and interictal bursts in prolonged intracranial recordings from epileptic canines. *Epilepsia*, 57(12):1949–1957, 2016. doi: 10.1111/epi.13591.
- Hoameng Ung, Steven N Baldassano, Hank Bink, Abba M Krieger, Shawniqua Williams, Flavia Vitale, Chengyuan Wu, Dean Freestone, Ewan Nurse, Kent Leyde, Kathryn A. Davis, Mark Cook, and Brian Litt. Intracranial EEG fluctuates over months after implanting electrodes in human brain. *Journal of Neural Engineering*, 14(5), 2017. ISSN 17412552. doi: 10.1088/1741-2552/aa7f40.
- Michael Wenzel, Jordan P. Hamm, Darcy S. Peterka, and Rafael Yuste. Reliable and elastic propagation of cortical seizures in vivo. *Cell Reports*, 19:2681–2693, 2017. ISSN 22111247. doi: 10.1016/j.celrep.2017.05.090.

Siqi Wu, Antony Joseph, Ann S. Hammonds, Susan E. Celniker, Bin Yu, and Erwin Frise. Stability-driven nonnegative matrix factorization to interpret spatial gene expression and build local gene networks. *Proceedings of the National Academy of Sciences*, 113(16):4290–4295, 2016. ISSN 0027-8424. doi: 10.1073/pnas.1521171113.

Xiaowei Zhuang, Zhengshi Yang, and Dietmar Cordes. A technical review of canonical correlation analysis for neuroscience applications. *Human Brain Mapping*, 41:3807–3833, 2020. ISSN 10970193. doi: 10.1002/hbm.25090.